

# VULCAN: Tool-Augmented Multi Agents for Iterative 3D Object Arrangement

Zhengfei Kuang<sup>1\*</sup>, Rui Lin<sup>2</sup>, Long Zhao<sup>2</sup>, Gordon Wetzstein<sup>1</sup>, Saining Xie<sup>2,3</sup>, Sanghyun Woo<sup>2</sup>

<sup>1</sup>Stanford University <sup>2</sup>Google <sup>3</sup>New York University

{zhengfei,gordonwz}@stanford.edu {linrui,shwoo}@google.com

gary.zhao9012@gmail.com saining.xie@nyu.edu

[vulcan-3d.github.io](https://vulcan-3d.github.io)

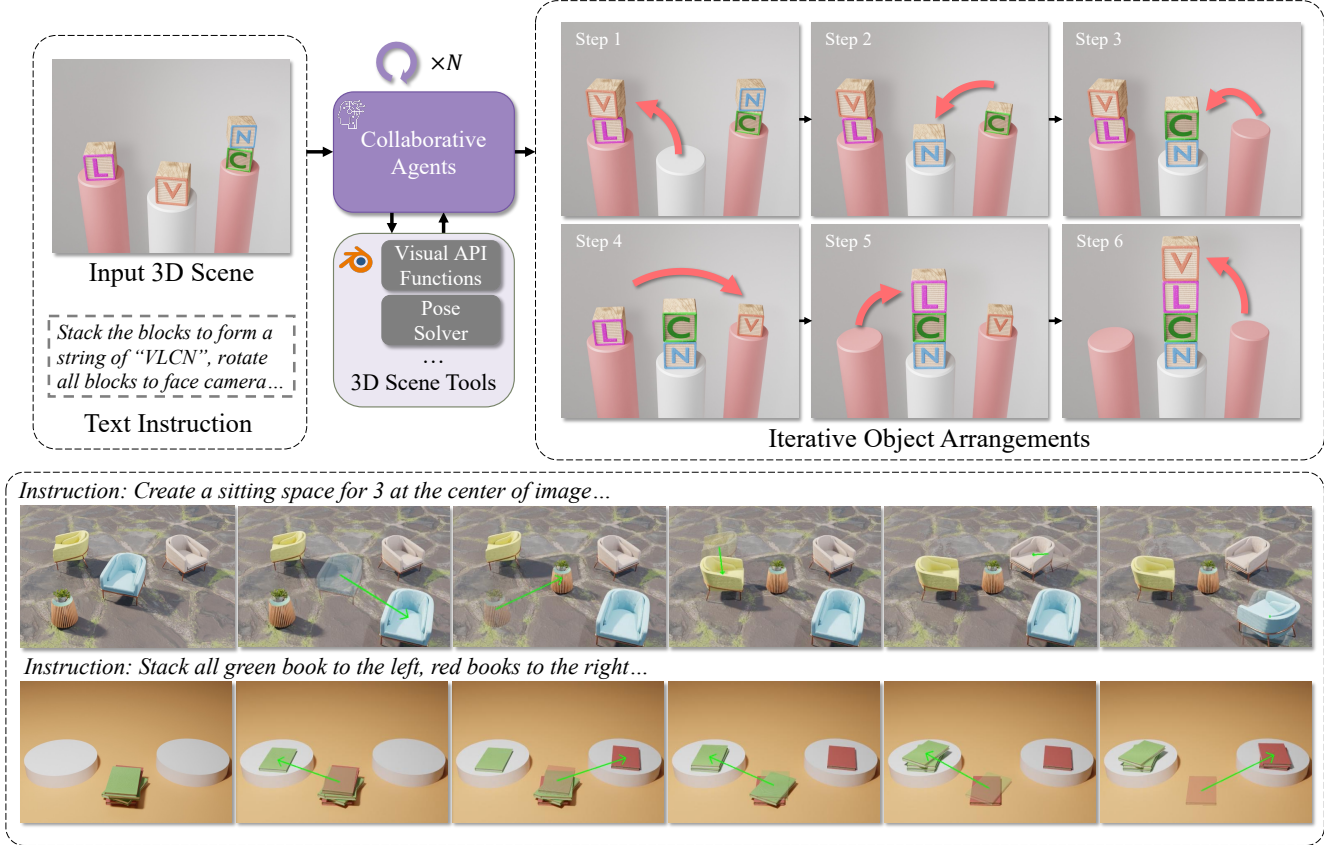


Figure 1. VULCAN plans and executes multiple actions for complex object arrangement tasks given input image and user prompt.

## Abstract

Despite the remarkable progress of Multimodal Large Language Models (MLLMs) in 2D vision-language tasks, their application to complex 3D scene manipulation remains underexplored. In this paper, we bridge this critical gap by

tackling three key challenges in 3D object arrangement task using MLLMs. First, to address the weak visual grounding of MLLMs, which struggle to link programmatic edits with precise 3D outcomes, we introduce an MCP-based API. This shifts the interaction from brittle raw code manipulation to more robust, function-level updates. Second, we augment the MLLM's 3D scene understanding with a suite

\*This work was done when Zhengfei Kuang was an intern at Google.

*of specialized visual tools to analyze scene state, gather spatial information, and validate action outcomes. This perceptual feedback loop is critical for closing the gap between language-based updates and precise 3D-aware manipulation. Third, to manage the iterative, error-prone updates, we propose a collaborative multi-agent framework with designated roles for planning, execution, and verification. This decomposition allows the system to robustly handle multi-step instructions and recover from intermediate errors. We demonstrate the effectiveness of our approach on a diverse set of 25 complex object arrangement tasks, where it significantly outperforms existing baselines.*

## 1. Introduction

Humans routinely rearrange objects in their environment, instinctively decomposing complex, multi-object tasks into sequential steps. For instance, moving a dining table naturally requires first clearing its surface and moving surrounding chairs. This fundamental ability to perform multi-step planning, grounded in deep spatial reasoning and a commonsense understanding of the physical world, is essential for executing complex arrangement tasks.

Recent Multimodal Large Language Models (MLLMs) [5, 34, 50, 56] have enhanced human-like reasoning, enabling prior works [14, 15, 21, 26, 27, 61] to explore 3D object arrangement, which involves moving, rotating, or inserting objects to create a plausible layout. However, a key limitation of these approaches is their formulation of arrangement as a single-step process: starting from an initial scene, the agent performs one comprehensive edit to reach the goal state. The standard pipeline simply involves MLLM agents analyzing the 3D scene to generate this single edit.

In this work, we introduce a fundamentally more flexible paradigm. The core of our approach is the ability to elastically decompose tasks. Our model is not confined to a single edit; instead it dynamically assesses the user’s instruction and the scene’s complexity. For simple requests, it can generate a single-step solution, similar to the capabilities of prior work. For complex tasks, it decomposes the instruction into a multi-step plan of sequential operations. This ability to decide whether to perform a single edit or long-horizon sequence of actions—a capability that was by design infeasible for previous approaches—is what allows our model to mirror the human-level reasoning and planning. Given a user instruction, whether abstract (e.g., “Create a dining space”) or detailed (e.g., “Move the book to the shelf, then move the table”), the agent can now formulate a coherent, step-by-step plan and reliably execute each action in sequence to achieve the specified goal.

The fundamental requirement for this advanced task is a pipeline that operates with high-fidelity and robustness at

every single step. In iterative arrangement, unlike single-step tasks, errors in either scene analysis or execution can propagate and compound, quickly derailing the entire multi-step process. Prior single-step approaches have employed various modalities for MLLM-based scene analysis, from raw visual representations [26, 27] to structured scene descriptions [24, 67]. However, these methods strike a poor balance: they either overburden the MLLM with complex raw 3D data it cannot natively parse or provide simplified information that is insufficient for robust spatial reasoning.

This is the gap that recent MLLM tool calling [28, 36, 62] and the development of the Model Context Protocol [23] have begun to address. These breakthroughs demonstrate a new way where MLLMs can be equipped to handle complex tasks [21, 46] that often lie beyond their core, encoded knowledge. This approach aids the MLLM by allowing to interact with external, use-defined application programming interfaces (APIs). Inspired by these innovations, we address both the analysis and execution challenges. For interactive analysis, we equip our agents with a powerful visual API toolset. This allows them to actively query the environment, infer scene layouts from observations, and determine appropriate arrangement configurations without being overburdened. For reliable execution, we develop an advanced collision-free solver. This component ensures physical plausibility by translating the agent’s high-level, symbolic intent into precise, valid numerical object poses.

The next critical challenge is scaling our tool-augmented capabilities to a multi-step scenario. This transition demands a sophisticated reasoning process: the agent must plan several moves ahead, ensuring each intermediate arrangement is not only physically plausible but also serves as a valid precondition for subsequent actions. Simultaneously managing high-level, long-horizon strategy and low-level, step-by-step execution is a significant burden for a single agent. We therefore separate these tasks by employing specialized agents with distinct responsibilities. One agent focuses on global planning across the entire task trajectory, while others handle the per-step execution and evaluation within the 3D scene. This division is implemented in our collaborative multi-agent pipeline.

Another critical challenge is the combinatorial search space. Multi-step arrangement is inherently complex; the search space grows exponentially with each step, as every placement decision branches into numerous possible future states. This creates a tree of possibilities that quickly becomes intractable. To manage this complexity, we propose an effective search algorithm that strategically backtracks from unpromising paths, efficiently pruning the search tree and avoiding the trap of exhaustive enumeration.

We propose **VULCAN**, a tailored agentic pipeline that leverages state-of-the-art MLLMs to generate accurate and plausible sequences of arrangements based on user instruc-

tions. We summarize our key contribution as:

- **A tool-augmented MLLM** that integrates MCP-based visual tools with a constraint-based solver for efficient 3D scene analysis and physically-plausible arrangement;
- **A collaborative multi-agent framework** that strategically separates responsibilities for global planning, step-by-step execution, and intermediate-state examination;
- **An adaptive backtracking search algorithm** that efficiently navigates the exponential search space to find a valid path to the goal state.
- **A new 3D object arrangement benchmark** designed to evaluate challenging 3D-aware object arrangements, on which our model significantly outperforms all the previous baselines.

## 2. Related Works

**3D Object Manipulation and Arrangement** The task of 3D object manipulation and arrangement is fundamental to both computer vision and robotics, as it enables agents to understand, interact with, and plausibly reorganize complex environments. Conventional 3D object arrangement methods typically employ large 3D datasets [11, 13, 32, 33, 43, 44, 60] to build data-driven models [16, 17, 52–55, 58]. However, these models are not guided by the common-sense reasoning of large language models, which limits their capability for general-purpose applications. Following recent developments in MLLMs [50, 56], recent works [15, 24, 49, 57, 61, 67] have begun to leverage the reasoning capabilities of MLLMs to address object arrangement in a way that aligns with common sense. Since the standard MLLMs are not natively trained on 3D scene data at scale, these works enable the MLLM to access various intermediate representations for 3D scene analysis, such as textual scene description files [12, 67], code scripts [26, 49], or rendered images [14, 26, 27]. Among these, FirePlace [27] and ScanEdit [14] also apply dedicated solvers with geometric constraints to ensure physically plausible results. However, all these works are limited to single-step operations. They lack the capability to handle complex multi-step scenarios where objects must be arranged sequentially with careful consideration of intermediate states. Our work directly addresses this gap by introducing an iterative framework that can decompose complex instructions into a coherent sequence of actions.

**MLLMs for 3D** The development of MLLMs extends large language models [50, 51, 56] to other modalities, including audio [18], image [5, 34], and video [7]. Leveraging their powerful cross-modal reasoning capabilities, numerous works have developed systems to tackle various vision-language-based 3D tasks, such as geometry generation [9, 38, 40, 47], scene understanding [6, 25, 39, 63, 65], and appearance editing [41, 48]. Compared to methods that

directly apply hard-coded algorithms [20, 30, 31, 35, 42, 64] or deep learning models on task-specific datasets [22, 45, 59, 66], these MLLM-based approaches demonstrate better generalization and produce more semantically plausible results. While benchmarks like BlenderGym [19] were introduced to evaluate these 3D operations, both these existing works and their benchmarks were not designed for complex object arrangement. They provide limited support for the spatial reasoning required by an iterative, multi-object scenario. In contrast, our framework is uniquely designed for this long-horizon arrangement task, and to properly validate this new, complex capability, we also introduce a novel benchmark including 25 distinct object manipulation scenarios specifically designed to thoroughly test multi-step planning and reasoning capability.

## 3. Problem Formulation

We formulate our problem as follows: Given an image  $I$  rendered from a fixed camera  $C$  in an underlying 3D scene  $S$ , and a textual instruction  $T$  (which may range from high-level goals to detailed per-step instructions), the model must output a sequence of single-object arrangements that accomplish the user’s objective while maintaining physical plausibility throughout all intermediate states.

We define three key objectives for these arrangements:

- **Collision-Free:** After each edit, the moved object should not collide with other objects in the scene.
- **Floating-Free:** After each edit, every object in the scene (except for those originally floating) should be placed solidly on a surface.
- **High Semantic Quality:** The arrangement should be semantically plausible and align well with the user’s intent.

Unlike existing work that focuses on single-object insertion or offline multi-object placement, our problem addresses sequential, multi-step movements. At each step, the model must comprehend the relationships between all sub-tasks and objects to devise a globally coherent and actionable plan, then execute it reliably to prevent unacceptable cumulative errors. Additionally, the model must effectively search across different solution branches to identify valid paths to the goal, and when necessary, recover from dead ends caused by previous missteps.

To address these challenges, we introduce several key innovations detailed in the following sections. Section 4 presents our collaborative MLLM agents for planning, placement, and evaluation; Section 5 describes our object arrangement framework, including API-based visual tools and a constraint-based collision-free solver; and Section 4 introduces our adaptive backtracking search algorithm for discovering valid multi-step plans.

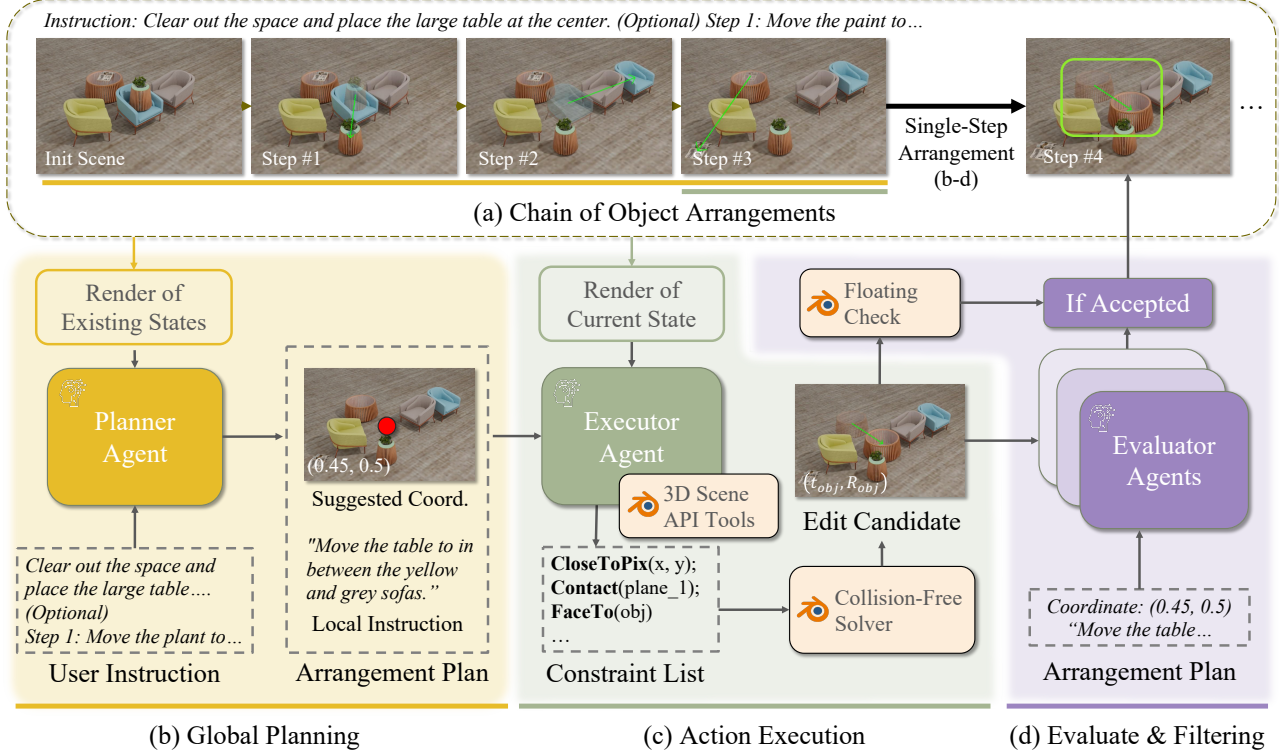


Figure 2. **VULCAN Overview.** (a) Our method solves a long-horizon task through an iterative multi-agent process. (b) The *Planner* agent examines the global context (the user instruction and all previous rendered states) to formulate a concrete plan for the current movement. (c) The *Executor* implements this single-step plan in the 3D scene using API tools and solvers. (d) A set of *Evaluators* and an automatic floating check assess the execution quality. The entire “Plan-Execute-Evaluate” loop repeats until the *Planner* validates that the final arrangement fulfills the original user instruction.

## 4. Multi-Agent Framework

Requiring a single MLLM to handle all 3D arrangement aspects introduces excessive processing burden and context length limitations. This problem is intensified in multi-step settings that demand global awareness. We therefore adopt a multi-agent approach with three specialized MLLMs [27, 48, 49]. Our pipeline (Figure 2) consists of three agents per step: the *Planner* extracts a concrete arrangement plan, the *Executor* operates the 3D scene using our framework, and the *Evaluator* validates the result. To effectively distribute the workload, this architecture has two key designs: First, the *Planner* receives global context (i.e., information from other steps), while the *Executor* and *Evaluator* operate only within the local scope of the current step. Second, only the *Executor* interacts directly with the 3D scene; the other two observe rendered images.

**Planning with Global Context** The *Planner* generates an executable action plan based on the user’s instruction and a visual history, which consists of sequential renderings from previous steps. It analyzes this visual timeline to understand

scene evolution and associates past states with the user’s goal to determine the most appropriate next action. Critically, the *Planner* outputs both a textual instruction and an approximate target placement as a normalized 2D pixel coordinate  $c = (x, y)$ . We found this combination of language and spatial grounding to generate a less ambiguous plan.

**Tool-Assisted Action Execution** To address the challenges of direct MLLM execution, which demands simultaneous instruction grounding, 3D modeling, and physical plausibility checks, our *Executor* defers these complexities to dedicated external modules. Specifically, we equip the MLLM with a suite of MCP-based APIs for interactive tool usage. The *Executor* leverages these tools to project the *Planner*’s instruction and 2D coordinate  $c$  into the 3D environment. The general execution pipeline proceeds as follows: First, it performs visual selection by querying the scene to localize a target object and receptacles. Next, it translates intended spatial relationships into a set of geometric constraints [14, 27]. Finally, the *Executor* invokes a optimization-based solver to compute an optimal, collision-free pose that guarantees physical validity. Details of our vi-

visual selection, constraint formulation, and solver optimization are presented in Sec. 5.

**Evaluation and Filtering** The final agent, the *Evaluator*, performs a visual check on the arrangement, examining its plausibility and consistency with the *Planner*’s instruction. Given the resulting image from the *Executor*, the agent provides one of five categorical ratings: terrible, bad, fair, good, or excellent. Due to the inherent uncertainty in current MLLMs, the *Evaluator* can occasionally produce hallucinated evaluations (e.g., giving an “excellent” rating to a completely incorrect placement). To mitigate this, we employ consensus-based filtering. This process involves polling multiple *Evaluator* agents and calculating an average judgment score, mapped from -2 (terrible) to +2 (excellent). A solution is only accepted if this consensus score is positive. Finally, in addition to the MLLM-based evaluation, we employ a rule-based check to detect physically implausible placements, such as floating objects. This deterministic check complements the agent’s learned judgment by catching obvious physical errors that a model might overlook. Any movement that violates these physical constraints is automatically rejected.

**Visual Annotation** To enhance agent reasoning, we augment input images with two features (Fig. 3). First, to provide precise spatial grounding, we add pixel coordinate labels and a dashed grid in the normalized pixel space. This grid helps the *Planner* to generate accurate target coordinates and for the *Executor* to ground its tools. Second, we visualize the completed action with an arrow connecting the object’s original location to its target. This clearly displays the start and end states, providing context for the *Planner* as it reviews the visual history and enabling the *Evaluator* to effectively assess the most recent edit.

**Adaptive Backtracking** During multi-step execution, errors from previous steps can render subsequent steps infeasible, leading to dead ends. For example, poor placement of initial objects on a table may leave insufficient space for later ones. To overcome this, we introduce an adaptive backtracking search algorithm, inspired by classic methods [10, 29], to efficiently recover from these errors. Our algorithm maintains an *anchor* step, which serves as the restart position for failed attempts. This anchor is adaptively reset: it moves to half the current depth when an attempt fails, or it advances when the action sequence reaches a new maximum length from the whole run (e.g. successfully placed three bottles on the table, while previous attempts placed at most two).

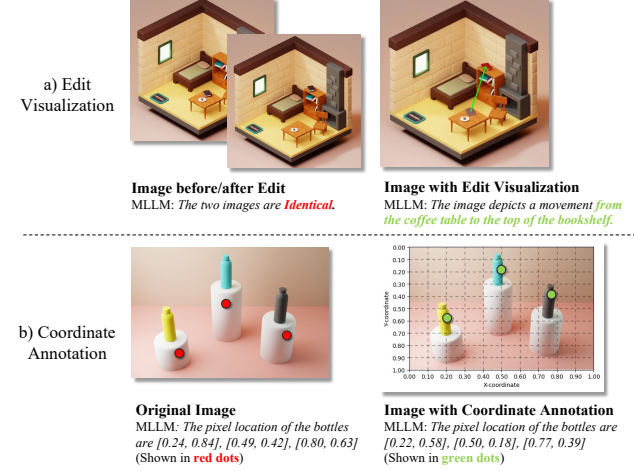


Figure 3. **Impact of visual annotation.** (a) Edit visualization improves the MLLM’s spatial arrangement recognition; (b) Coordinate annotations enhance its object localization accuracy.

## 5. Multi-Tool Library

As described in Sec. 4, the *Executor* agent’s primary role is to translate the *Planner*’s 2D-based instruction into a physically valid 3D action. To bridge this 2D-to-3D gap, the *Executor* is equipped with a visual tool library that defines a clear, step-by-step workflow:

1. **Visual Probing:** The agent queries the 3D scene to “see” and identify the 3D objects and planes.
2. **Constraint Formulation:** The agent assembles a placement plan as a list of geometric constraints.
3. **Optimization:** The constraints are passed to a solver, which computes the optimal valid 3D pose.

**Visual Probing** We equip the agent with three visual probing tools, to interactively analyze the 3D scene layout.

- **LISTOBJECTSINAREA:** Returns object names within or partially overlapping a specified image area. This helps the MLLM identify objects visible in that region.
- **RAYPROBE:** Casts a ray from the camera at a given pixel coordinate and returns information about the first hit point. This includes the 3D location, the name of the hit object, and the name and normal of the hit plane.
- **RENDERWITHHIGHLIGHT:** Renders an instance segmentation image with specified objects highlighted. This function helps the MLLM confirm the correlation between object names and their visual representations.

During a typical *Executor* run, we observe that the agent calls **LISTOBJECTSINAREA** and **RAYPROBE** to retrieve the names of relevant objects and planes, including the object to be edited and any reference objects. If the name alone is ambiguous (e.g., multiple objects named “Book”),

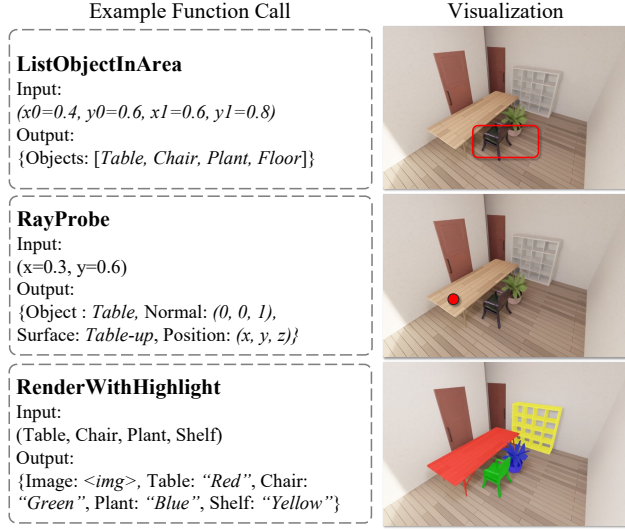


Figure 4. **Visual Probing Tools.** For each API, we present an example function call format, along with a result visualization.

the agent will then call **RENDERTWITHHIGHLIGHT** to visually discern the correct target object from the others.

**Constraint Formulation** After identifying the necessary 3D elements, the agent assembles a placement plan as a list of constraints. The supported constraints are:

- **CLOSETOPIX**( $obj, x, y$ ): The placed object  $obj$  should be located close to the pixel coordinate  $(x, y)$  in camera  $C$ 's view.
- **CONTACT**( $obj, dir, p$ ): The plane of the object  $obj$ 's bounding box facing  $dir$  should contact the plane  $p$ .
- **NOOVERHANG**( $obj, dir, p$ ): The plane of the object's bounding box facing  $dir$  should be fully inside the convex hull of plane  $p$ .
- **DISTANCE**( $obj, obj_2, dist$ ): The Euclidean distance between  $obj$  and  $obj_2$  should be close to  $dist$ .
- **FACETO**( $obj, obj_2/p$ ): The facing direction of object  $obj$  should point towards the center of  $obj_2$ , or align with the normal direction of plane  $p$ .
- **ROTATE**( $obj, degree$ ): The object should rotate counter-clockwise by  $degree$ .

Together, these constraints form a comprehensive vocabulary that ensures strong geometric plausibility and is applicable to a wide variety of 3D object arrangement tasks.

**Optimization** Given that the target pixel  $c$  and constraints from previous steps already define a small search space, we adopt an efficient, sampling-based approach. Inspired by preconditioning techniques in numerical analysis [4, 8], we first randomly perturb the target pixel coordinate  $c$  into a batch of variants. Next, we apply the solver to each variant, generating a set of candidate poses distributed around

the original target. The solver employs an AdamW [37] optimizer to minimize constraint losses. Following optimization, we validate each solved candidate by recalculating its constraint losses in the original pixel coordinate space, and remove any candidates whose error exceeds the threshold  $\tau$ . Finally, a collision detector filters these candidates, and we select the valid, collision-free pose with the lowest constraint error. This method, detailed in Alg. 1, efficiently ensures a non-colliding solution.

#### Algorithm 1: Constraint-based Pose Solver

---

**Parameter:** pixel coordinate variance  $\sigma_{pix}$ , loss threshold  $\tau$

**Input:** Suggested pixel coordinate  $c$ , Constraint list  $D = \{d_1, \dots, l\}$

**Output:** The target object pose  $T_{obj} = (t_{obj}, R_{obj})$   
 $c'_{1, \dots, n} \leftarrow \text{Sample}(\mathcal{N}(c, \sigma_{pix}))$ ;  
 $T_{1, \dots, n} \leftarrow \text{Optimize}(D, c'_{1, \dots, n})$ ;  
/\* Pre-filtering with constraint errors \*/  
 $T_{1, \dots, m}^{pre} \leftarrow \text{FilterByError}(T_{1, \dots, n}, D, c, \tau)$ ;  
**for**  $T_i$  in  $\text{SortByError}(T_{1, \dots, m}^{pre})$  **do**  
|   **if** not  $\text{CollisionDetected}(T_i)$  **then**  
|   |   **return**  $T_i$ ;  
**end**  
**return** "Failed";

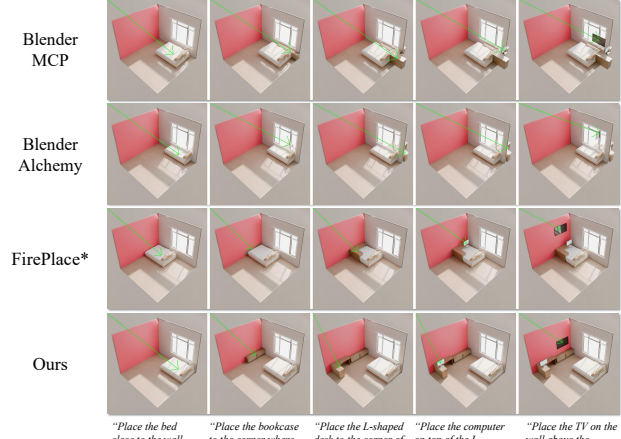
---

## 6. Experiments

We conduct all experiments using Gemini-2.5-pro, a state-of-the-art MLLM. Our object arrangement framework, including the constraint-based solver and API visual functions, is implemented using Blender's Python extension packages integrated with the Blender-MCP library [3]. For each arrangement step, we employ 3 *Evaluator* agents and execute 4 parallel attempts, selecting the valid solution with the highest average evaluation score. If no solution is found in all attempts, the step is marked as failed and the system proceeds with backtracking.

### 6.1. Dataset and Metrics

We evaluate our model's ability to produce plausible and precise multi-step arrangements through comprehensive benchmark comparisons against baseline approaches. Our evaluation dataset comprises 25 carefully curated scenes sourced from BlenderKit [2], InfiniGen [43, 44], and BlenderGym [19], encompassing 111 unit tasks in total. To ensure fair comparison, all baseline methods receive identical reference per-step instructions and execute the same sequence of operations. The task design deliberately introduces interdependencies where subsequent steps can be affected by preceding operations without proper execution.



(a) Benchmark Comparison (Per-Step Instruction)

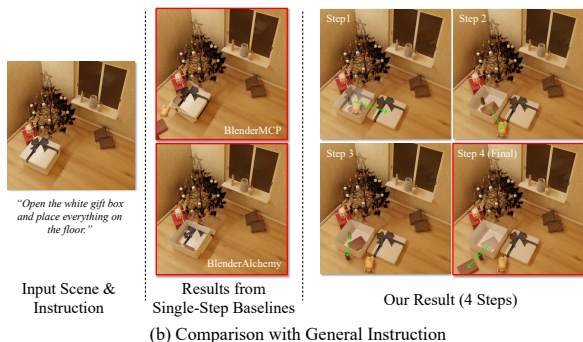


Figure 5. **Qualitative Comparisons.** We compare results using two types of guidance: detailed per-step instructions (*Top*) and general, abstract instructions (*Bottom*). *Top*: When given per-step instructions, our method outperforms the baselines. *Bottom*: Using general instructions, our multi-step approach produces reasonable intermediate states and yields a significantly better final state (marked in red) compared to single-step baselines.

We assess performance at every step using the following metrics, averaged across all tasks:

- **Collision Rate:** The proportion of steps that result in a collision between the moved object and other elements.
- **Floating Rate:** The proportion of steps that cause any object in the scene to become unsupported (i.e., “floating”).
- **Plausibility:** The physical realism of the arrangement, assessed by an MLLM, scored from 0 (poor) to 4 (great).
- **Consistency:** The alignment between the user’s instructions and the resulting arrangement, assessed by an MLLM and scored from 0 to 4.

## 6.2. Baselines Comparisons

We compare our **VULCAN** against three recent MLLM-based approaches, selected to represent different components of our system: **BlenderAlchemy** [26] employs MLLM agents in an executor-evaluator loop to edit Blender

Method	Coll.% $\downarrow$	Fl.% $\downarrow$	Plausibility $\uparrow$	Consistency $\uparrow$
Blender-MCP	0.459	0.774	3.348	2.973
BlenderAlchemy	0.631	0.676	3.368	2.770
FirePlace*	0.513	0.225	3.515	3.135
Ours	<b>0.000</b>	<b>0.000</b>	<b>3.796</b>	<b>3.592</b>

Table 1. **Quantitative Comparisons.** We compare our method against baselines using several metrics: the average rate of collision (*Coll.%*), the rate of floating (*Fl.%*), visual plausibility score (*Plausibility*), and a consistency score between the text instruction and edited image (*Consistency*).

scenes via Python scripts. This aligns with parts of our multi-agent structure but lacks the interactive visual tools and constraint-based solver used by our Executor agent. We provide object poses as input to its script representation. **Fireplace** [27] represents the state-of-the-art in using a constraint-based solver with MLLMs for object placement, which is analogous to our Executor’s core solving capability. However, it operates as a standalone solver and lacks our system’s broader multi-agent framework (i.e., the Planner and Evaluator agents) for global context and multi-step reasoning. We reimplemented the method for our setting. **Blender-MCP** [3] enables MLLM interaction with 3D scenes through basic callable functions (GETSCENEINFO, GETOBJECTINFO, RENDERIMAGE, and EXECUTECODE), representing a simpler, tool-only baseline. It lacks our framework’s specialized agent roles (Planner, Evaluator), constraint-based solver, and multi-step reasoning capabilities. We configure this baseline to use its default function set.

Table 1 presents the quantitative results, demonstrating that our approach substantially outperforms all baselines. Our method not only generates more realistic and accurate movements but also precisely eliminates collisions and floating artifacts, thanks to our collision-free solver and filter techniques. Figure 5 shows qualitative comparisons on benchmark and general instruction examples. In the first example, BlenderAlchemy and Blender-MCP fail completely without effective API tools and solvers. Fireplace successfully moves the bed but subsequent placements collide with it. Our method achieves artifact-free results. In the second example, single-step baselines fail on complex tasks, while our multi-step approach produces high-quality results.

## 6.3. Human Evaluation

In addition to MLLM evaluations, we also conduct a human study involving 30 subjects for evaluating our models with baselines. Specifically, we provide the result of our model and result of the baselines, and let the subjects to decide

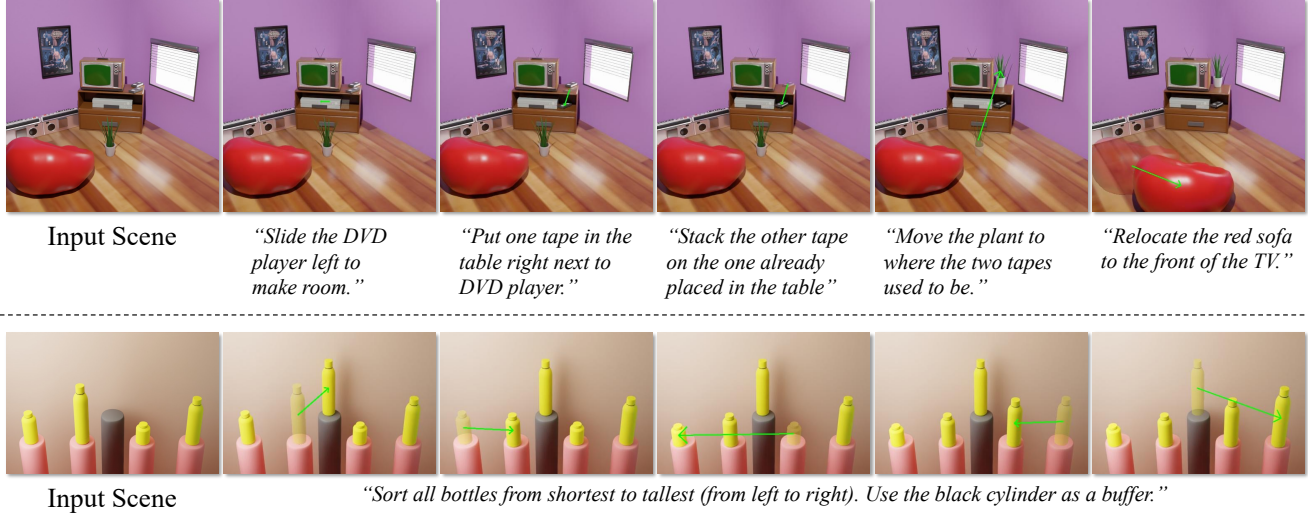


Figure 6. **More Visual Results.** Our model tackles complex arrangement tasks with per-step prompts (top) or general instructions (bottom).

which one looks more physically correct, visually plausible and consistent to the instructions. We collect the winning rate of our model competing with each baselines. As Tab. 2 shows, users generally prefer our models's result than the others with a huge margin.

Method	Win % / Tie %		
	Const.	Plaus.	Phys.
Ours vs. BlenderAlchemy [26]	<b>62.1</b> /22.7	<b>65.9</b> /24.7	<b>70.0</b> /20.0
Ours vs. Blender-MCP [3]	<b>60.5</b> /25.0	<b>59.0</b> /25.8	<b>62.9</b> /26.1
Ours vs. FirePlace* [27]	<b>58.8</b> /30.2	<b>54.4</b> /35.0	<b>58.0</b> /31.5

Table 2. **Results on Human Study.** We conduct a human study to compare our model with baselines on three domains: Instruction Following (*Const.*), Visual Plausibility (*Plaus.*) and Physical Plausibility (*Phys.*). Our model is significantly more favorable to the users than the baselines in all aspects. We re-implemented Fireplace with adaptation to our task since its code is not released.

#### 6.4. Ablation Study

We conduct ablation experiments on the same benchmark to validate the contribution of each architectural component. We compare our full model against five variants: **Model w/o Multi Tool Library** removes the constraint-based solver and visual API, using Blender-MCP [3] functions instead. **Model w/o Backtracking** eliminates adaptive backtracking and always proceeds to the next step, selecting the best solution even with artifacts (solver allows collisions). **Model w/o MCP Tools** variant removes all tools requiring MCP [23] (including the original Blender-MCP [3] functions). Instead, it requires the model to directly predict raw Blender [1] Python scripts for object arrangement. **Model**

Method	Coll.% $\downarrow$	Fl.% $\downarrow$	Plaus. $\uparrow$	Const. $\uparrow$
w/o Multi-Tool Library	0.495	0.711	3.484	3.103
w/o Backtracking	0.036	0.054	3.703	3.549
w/o MCP Tools	0.603	0.738	3.357	3.067
w/o Planner's Coordinates	<b>0.000</b>	<b>0.000</b>	3.772	3.526
Single Agent	<b>0.000</b>	<b>0.000</b>	3.623	3.328
Ours	<b>0.000</b>	<b>0.000</b>	<b>3.796</b>	<b>3.592</b>

Table 3. **Ablation Study Results.** Our complete model achieves substantially better performance than any ablated variant.

**w/o Planner Coordinates** variant removes coordinate guidance from the *Planner* agent. **Model w/ Single Agent** replaces our collaborative multi-agent system with a single MLLM agent.

Table 3 demonstrates that the complete model achieves optimal performance across all metrics. Removing the solver and visual tools substantially degrades plausibility and quality, though performance still exceeds the original Blender-MCP baseline due to our multi-agent design and backtracking mechanism. Without backtracking, the model occasionally accepts suboptimal solutions, resulting in small but non-zero collision and floating rates—though the overall pipeline robustness keeps these occurrences rare in the benchmark. The single-agent variant maintains zero collision and floating artifacts but exhibits reduced visual quality and textual consistency, confirming the importance of our multi-agent decomposition for preserving reasoning quality in complex multi-step scenarios.

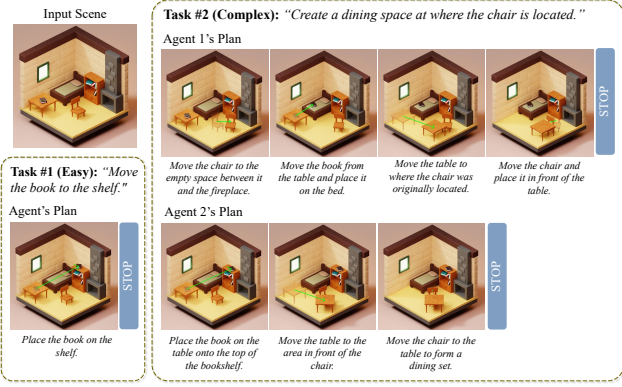


Figure 7. **Adaptive Planning.** Our model plans adaptively for different tasks and can generate diverse plans for the same objective. The plan output is shown below the corresponding edited image.

## 6.5. Visual Results

We present additional qualitative results demonstrating our method’s performance across various tasks. Figure 6 illustrates our model’s ability to handle complex scenarios requiring robust placement pipelines and effective global reasoning across multiple steps. Figure 7 further demonstrates the model’s flexibility in generating diverse plans: It adapts its planning to different tasks and produces diverse solutions for identical objectives across runs.

## 7. Conclusion

We propose **VULCAN**, a robust iterative object arrangement pipeline that addresses multi-step 3D arrangement tasks from textual input. Equipped with novel visual API tools, a collision-free solver, collaborative agents, and adaptive backtracking, our model effectively handles complex tasks and substantially outperforms state-of-the-art baselines. Meanwhile, to maintain optimal MLLM reasoning performance with reasonable context length, our current system is designed to support single-camera views only. This limits performance on tasks requiring novel view observations, for example, placing a chair to the unseen space behind a wall. We believe our pipeline can be extended to multi-view scenarios as long-context MLLMs continue to develop.

## 7.1. Acknowledgement

This work was supported by computational resources provided by Google Cloud. We thank Alireza Fathi, Yanan Bao, and Ian Huang for their assistance in reproducing the results from Fireplace, as well as Jiacheng Chen for his technical support with Blender scripting.

## References

- [1] Blender. <https://www.blender.org/>, . 8, 1
- [2] Blenderkit. <https://www.blenderkit.com/>, . 6
- [3] Blender-mcp. <https://github.com/ahujasid/blender-mcp?tab=readme-ov-file>, . 6, 7, 8, 1
- [4] Owe Axelsson. *Iterative Solution Methods*. Cambridge University Press, 1994. 6
- [5] Shuai Bai, Keqin Chen, Xuejing Liu, Jialin Wang, Wenbin Ge, Sibo Song, Kai Dang, Peng Wang, Shijie Wang, Jun Tang, et al. Qwen2. 5-vl technical report. *arXiv preprint arXiv:2502.13923*, 2025. 2, 3
- [6] Boyuan Chen, Zhuo Xu, Sean Kirmani, Brain Ichter, Dorsa Sadigh, Leonidas Guibas, and Fei Xia. Spatialvlm: Endowing vision-language models with spatial reasoning capabilities. In *Proceedings of the IEEE/CVF Conference on Computer Vision and Pattern Recognition*, pages 14455–14465, 2024. 3
- [7] Guo Chen, Yin-Dong Zheng, Jiahao Wang, Jilan Xu, Yifei Huang, Junting Pan, Yi Wang, Yali Wang, Yu Qiao, Tong Lu, et al. Videollm: Modeling video sequence with large language models. *arXiv preprint arXiv:2305.13292*, 2023. 3
- [8] Ke Chen. *Matrix Preconditioning Techniques and Applications*. Cambridge University Press, 2005. 6
- [9] Tianrun Chen, Chunyan Yu, Yuanqi Hu, Jing Li, Tao Xu, Runlong Cao, Lanyun Zhu, Ying Zang, Yong Zhang, Zejian Li, et al. Img2cad: Conditioned 3-d cad model generation from single image with structured visual geometry. *IEEE Transactions on Industrial Informatics*, 2025. 3
- [10] Dah-Ming Chiu and Raj Jain. Analysis of the increase and decrease algorithms for congestion avoidance in computer networks. *Computer Networks and ISDN systems*, 17(1):1–14, 1989. 5
- [11] Angela Dai, Angel X. Chang, Manolis Savva, Maciej Halber, Thomas Funkhouser, and Matthias Nießner. Scannet: Richly-annotated 3d reconstructions of indoor scenes. In *Proc. Computer Vision and Pattern Recognition (CVPR), IEEE*, 2017. 3
- [12] Fernanda De La Torre, Cathy Mengying Fang, Han Huang, Andrzej Banburski-Fahey, Judith Amores Fernandez, and Jaron Lanier. Llmr: Real-time prompting of interactive worlds using large language models. In *Proceedings of the 2024 CHI Conference on Human Factors in Computing Systems*, pages 1–22, 2024. 3
- [13] Matt Deitke, Eli VanderBilt, Alvaro Herrasti, Luca Weihs, Kiana Ehsani, Jordi Salvador, Winson Han, Eric Kolve, Aniruddha Kembhavi, and Roozbeh Mottaghi. Procthor: Large-scale embodied ai using procedural generation. *Advances in Neural Information Processing Systems*, 35:5982–5994, 2022. 3
- [14] Mohamed el amine Boudjoghra, Ivan Laptev, and Angela Dai. Scannedit: Hierarchically-guided functional 3d scan editing, 2025. 2, 3, 4
- [15] Weixi Feng, Wanrong Zhu, Tsu-jui Fu, Varun Jampani, Arjun Akula, Xuehai He, Sugato Basu, Xin Eric Wang, and William Yang Wang. Layoutgpt: Compositional visual planning and generation with large language models. *arXiv preprint arXiv:2305.15393*, 2023. 2, 3

[16] Matthew Fisher, Daniel Ritchie, Manolis Savva, Thomas Funkhouser, and Pat Hanrahan. Example-based synthesis of 3d object arrangements. In *ACM SIGGRAPH Asia 2012 papers*, 2012. 3

[17] Matthew Fisher, Manolis Savva, Yangyan Li, Pat Hanrahan, and Matthias Nießner. Activity-centric scene synthesis for functional 3d scene modeling. *ACM Transactions on Graphics (TOG)*, 34(6):1–13, 2015. 3

[18] Sreyan Ghosh, Sonal Kumar, Ashish Seth, Chandra Kiran Reddy Evuru, Utkarsh Tyagi, S Sakshi, Oriol Nieto, Ramani Duraiswami, and Dinesh Manocha. Gama: A large audio-language model with advanced audio understanding and complex reasoning abilities. *arXiv preprint arXiv:2406.11768*, 2024. 3

[19] Yunqi Gu, Ian Huang, Jihyeon Je, Guandao Yang, and Leonidas Guibas. Blendergym: Benchmarking foundational model systems for graphics editing. In *Proceedings of the Computer Vision and Pattern Recognition Conference*, pages 18574–18583, 2025. 3, 6

[20] Ayaan Haque, Matthew Tancik, Alexei Efros, Aleksander Holynski, and Angjoo Kanazawa. Instruct-nerf2nerf: Editing 3d scenes with instructions. In *Proceedings of the IEEE/CVF International Conference on Computer Vision*, 2023. 3

[21] Shun-ichiro Hayashi, Daichi Mukunoki, Tetsuya Hoshino, Satoshi Ohshima, and Takahiro Katagiri. 3dify: a framework for procedural 3d-cg generation assisted by llms using mcp and rag. *arXiv preprint arXiv:2510.04536*, 2025. 2

[22] Yicong Hong, Kai Zhang, Juxiang Gu, Sai Bi, Yang Zhou, Difan Liu, Feng Liu, Kalyan Sunkavalli, Trung Bui, and Hao Tan. Lrm: Large reconstruction model for single image to 3d. *arXiv preprint arXiv:2311.04400*, 2023. 3

[23] Xinyi Hou, Yanjie Zhao, Shenao Wang, and Haoyu Wang. Model context protocol (mcp): Landscape, security threats, and future research directions. *arXiv preprint arXiv:2503.23278*, 2025. 2, 8

[24] Ziniu Hu, Ahmet Iscen, Aashi Jain, Thomas Kipf, Yisong Yue, David A Ross, Cordelia Schmid, and Alireza Fathi. Scenecraft: An llm agent for synthesizing 3d scenes as blender code. In *Forty-first International Conference on Machine Learning*, 2024. 2, 3

[25] Haifeng Huang, Yilun Chen, Zehan Wang, Rongjie Huang, Runsen Xu, Tai Wang, Luping Liu, Xize Cheng, Yang Zhao, Jiangmiao Pang, et al. Chat-scene: Bridging 3d scene and large language models with object identifiers. *Advances in Neural Information Processing Systems*, 37: 113991–114017, 2024. 3

[26] Ian Huang, Guandao Yang, and Leonidas Guibas. Blender-alchemy: Editing 3d graphics with vision-language models. In *European Conference on Computer Vision*, pages 297–314. Springer, 2024. 2, 3, 7, 8, 1

[27] Ian Huang, Yanan Bao, Karen Truong, Howard Zhou, Cordelia Schmid, Leonidas Guibas, and Alireza Fathi. Fireplace: Geometric refinements of llm common sense reasoning for 3d object placement. *arXiv preprint arXiv:2503.04919*, 2025. 2, 3, 4, 7, 8

[28] Sehoon Kim, Suhong Moon, Ryan Tabrizi, Nicholas Lee, Michael W. Mahoney, Kurt Keutzer, and Amir Gholami. An LLM compiler for parallel function calling. In *Proceedings of the 41st International Conference on Machine Learning*, pages 24370–24391. PMLR, 2024. 2

[29] Donald E Knuth, James H Morris, Jr, and Vaughan R Pratt. Fast pattern matching in strings. *SIAM journal on computing*, 6(2):323–350, 1977. 5

[30] Zhengfei Kuang, Kyle Olszewski, Menglei Chai, Zeng Huang, Panos Achlioptas, and Sergey Tulyakov. Neroic: Neural rendering of objects from online image collections. *ACM Transactions on Graphics (TOG)*, 41(4):1–12, 2022. 3

[31] Zhengfei Kuang, Fujun Luan, Sai Bi, Zhixin Shu, Gordon Wetzstein, and Kalyan Sunkavalli. Palettenerf: Palette-based appearance editing of neural radiance fields. In *Proceedings of the IEEE/CVF Conference on Computer Vision and Pattern Recognition*, pages 20691–20700, 2023. 3

[32] Jiaman Li, Jiajun Wu, and C Karen Liu. Object motion guided human motion synthesis. *ACM Transactions on Graphics (TOG)*, 42(6):1–11, 2023. 3

[33] Jiaman Li, Alexander Clegg, Roozbeh Mottaghi, Jiajun Wu, Xavier Puig, and C Karen Liu. Controllable human-object interaction synthesis. In *European Conference on Computer Vision*, pages 54–72. Springer, 2024. 3

[34] Haotian Liu, Chunyuan Li, Qingyang Wu, and Yong Jae Lee. Visual instruction tuning. *Advances in neural information processing systems*, 36:34892–34916, 2023. 2, 3

[35] Steven Liu, Xiuming Zhang, Zhoutong Zhang, Richard Zhang, Jun-Yan Zhu, and Bryan Russell. Editing conditional radiance fields. In *Proceedings of the IEEE/CVF international conference on computer vision*, pages 5773–5783, 2021. 3

[36] Weiwen Liu, Xu Huang, Xingshan Zeng, Xinlong Hao, Shuai Yu, Dexun Li, Shuai Wang, Weinan Gan, Zhengying Liu, Yuanqing Yu, Zezhong Wang, Yuxian Wang, Wu Ning, Yutai Hou, Bin Wang, Chuhan Wu, Xinzhi Wang, Yong Liu, Yasheng Wang, Duyu Tang, Dandan Tu, Lifeng Shang, Xin Jiang, Ruiming Tang, Defu Lian, Qun Liu, and Enhong Chen. Toolace: Winning the points of llm function calling. *ArXiv*, abs/2409.00920, 2024. 2

[37] Ilya Loshchilov and Frank Hutter. Decoupled weight decay regularization. In *International Conference on Learning Representations*, 2017. 6

[38] Sining Lu, Guan Chen, Nam Anh Dinh, Itai Lang, Ari Holtzman, and Rana Hanocka. Ll3m: Large language 3d models, 2025. 3

[39] Muhammad Maaz, Hanoona Rasheed, Salman Khan, and Fahad Shahbaz Khan. Videogpt+: Integrating image and video encoders for enhanced video understanding. *arxiv*, 2024. 3

[40] Kiyohiro Nakayama, Jan Ackermann, Timur Levent Kesdogan, Yang Zheng, Maria Korosteleva, Olga Sorkine-Hornung, Leonidas J Guibas, Guandao Yang, and Gordon Wetzstein. Aipparel: A multimodal foundation model for digital garments. In *Proceedings of the Computer Vision and Pattern Recognition Conference*, pages 8138–8149, 2025. 3

[41] Francesco Palandra, Andrea Sanchietti, Daniele Baieri, and Emanuele Rodola. Gsedit: Efficient text-guided editing of 3d objects via gaussian splatting. *arXiv preprint arXiv:2403.05154*, 2024. 3

[42] Ben Poole, Ajay Jain, Jonathan T Barron, and Ben Mildenhall. Dreamfusion: Text-to-3d using 2d diffusion. *arXiv preprint arXiv:2209.14988*, 2022. 3

[43] Alexander Raistrick, Lahav Lipson, Zeyu Ma, Lingjie Mei, Mingzhe Wang, Yiming Zuo, Karhan Kayan, Hongyu Wen, Beining Han, Yihan Wang, Alejandro Newell, Hei Law, Ankit Goyal, Kaiyu Yang, and Jia Deng. Infinite photorealistic worlds using procedural generation. In *Proceedings of the IEEE/CVF Conference on Computer Vision and Pattern Recognition*, pages 12630–12641, 2023. 3, 6

[44] Alexander Raistrick, Lingjie Mei, Karhan Kayan, David Yan, Yiming Zuo, Beining Han, Hongyu Wen, Meenal Parakh, Stamatios Alexandropoulos, Lahav Lipson, et al. Infinigen indoors: Photorealistic indoor scenes using procedural generation. In *Proceedings of the IEEE/CVF Conference on Computer Vision and Pattern Recognition*, pages 21783–21794, 2024. 3, 6

[45] Xuanchi Ren, Jiahui Huang, Xiaohui Zeng, Ken Museth, Sanja Fidler, and Francis Williams. Xcube: Large-scale 3d generative modeling using sparse voxel hierarchies. In *Proceedings of the IEEE/CVF conference on computer vision and pattern recognition*, pages 4209–4219, 2024. 3

[46] Haozhan Shen, Kangjia Zhao, Tiancheng Zhao, Ruochen Xu, Zilun Zhang, Mingwei Zhu, and Jianwei Yin. ZoomEye: Enhancing multimodal LLMs with human-like zooming capabilities through tree-based image exploration. In *Proceedings of the 2025 Conference on Empirical Methods in Natural Language Processing*, pages 6613–6629, Suzhou, China, 2025. Association for Computational Linguistics. 2

[47] Yawar Siddiqui, Antonio Alliegro, Alexey Artemov, Tatiana Tommasi, Daniele Sirigatti, Vladislav Rosov, Angela Dai, and Matthias Nießner. Meshgpt: Generating triangle meshes with decoder-only transformers. In *Proceedings of the IEEE/CVF conference on computer vision and pattern recognition*, pages 19615–19625, 2024. 3

[48] Chunyi Sun, Junlin Han, Weijian Deng, Xinlong Wang, Zishan Qin, and Stephen Gould. 3d-gpt: Procedural 3d modeling with large language models. In *2025 International Conference on 3D Vision (3DV)*, pages 1253–1263. IEEE, 2025. 3, 4

[49] Fan-Yun Sun, Weiyu Liu, Siyi Gu, Dylan Lim, Goutam Bhat, Federico Tombari, Manling Li, Nick Haber, and Jiajun Wu. Layoutvlm: Differentiable optimization of 3d layout via vision-language models. In *Proceedings of the Computer Vision and Pattern Recognition Conference*, pages 29469–29478, 2025. 3, 4

[50] Gemini Team, Rohan Anil, Sebastian Borgeaud, Jean-Baptiste Alayrac, Jiahui Yu, Radu Soricut, Johan Schalkwyk, Andrew M Dai, Anja Hauth, Katie Millican, et al. Gemini: a family of highly capable multimodal models. *arXiv preprint arXiv:2312.11805*, 2023. 2, 3

[51] Hugo Touvron, Thibaut Lavril, Gautier Izacard, Xavier Martinet, Marie-Anne Lachaux, Timothée Lacroix, Baptiste Rozière, Naman Goyal, Eric Hambro, Faisal Azhar, et al. Llama: Open and efficient foundation language models. *arXiv preprint arXiv:2302.13971*, 2023. 3

[52] Kai Wang, Manolis Savva, Angel X Chang, and Daniel Ritchie. Deep convolutional priors for indoor scene synthesis. *ACM Transactions on Graphics (TOG)*, 37(4):1–14, 2018. 3

[53] Kai Wang, Yu-An Lin, Ben Weissmann, Manolis Savva, Angel X Chang, and Daniel Ritchie. Planit: Planning and instantiating indoor scenes with relation graph and spatial prior networks. *ACM Transactions on Graphics (TOG)*, 38(4):1–15, 2019.

[54] Xinpeng Wang, Chandan Yeshwanth, and Matthias Nießner. Sceneformer: Indoor scene generation with transformers. In *2021 International Conference on 3D Vision (3DV)*, pages 106–115. IEEE, 2021.

[55] QiuHong Anna Wei, Sijie Ding, Jeong Joon Park, Rahul Sajnani, Adrien Poulenard, Srinath Sridhar, and Leonidas Guibas. Lego-net: Learning regular rearrangements of objects in rooms. In *Proceedings of the IEEE/CVF Conference on Computer Vision and Pattern Recognition*, pages 19037–19047, 2023. 3

[56] Philip Welsby and Bernard MY Cheung. Chatgpt, 2023. 2, 3

[57] Zhen Wu, Jiaman Li, Pei Xu, and C Karen Liu. Human-object interaction from human-level instructions. In *Proceedings of the IEEE/CVF International Conference on Computer Vision*, pages 11176–11186, 2025. 3

[58] Kun Xu, Kang Chen, Hongbo Fu, Wei-Lun Sun, and Shi-Min Hu. Sketch2scene: Sketch-based co-retrieval and co-placement of 3d models. *ACM Transactions on Graphics (TOG)*, 32(4):1–15, 2013. 3

[59] Yinghao Xu, Menglei Chai, Zifan Shi, Sida Peng, Ivan Skorokhodov, Aliaksandr Siarohin, Ceyuan Yang, Yujun Shen, Hsin-Ying Lee, Bolei Zhou, et al. Discoscene: Spatially disentangled generative radiance fields for controllable 3d-aware scene synthesis. In *Proceedings of the IEEE/CVF conference on computer vision and pattern recognition*, pages 4402–4412, 2023. 3

[60] Jianing Yang, Xuweiyi Chen, Nikhil Madaan, Madhavan Iyengar, Shengyi Qian, David F Fouhey, and Joyce Chai. 3d-grand: A million-scale dataset for 3d-llms with better grounding and less hallucination. In *Proceedings of the Computer Vision and Pattern Recognition Conference*, pages 29501–29512, 2025. 3

[61] Yue Yang, Fan-Yun Sun, Luca Weihs, Eli VanderBilt, Alvaro Herrasti, Winson Han, Jiajun Wu, Nick Haber, Ranjay Krishna, Lingjie Liu, et al. Holodeck: Language guided generation of 3d embodied ai environments. In *Proceedings of the IEEE/CVF Conference on Computer Vision and Pattern Recognition*, pages 16227–16237, 2024. 2, 3

[62] Shunyu Yao, Jeffrey Zhao, Dian Yu, Nan Du, Izhak Shafran, Karthik Narasimhan, and Yuan Cao. ReAct: Synergizing reasoning and acting in language models. In *International Conference on Learning Representations (ICLR)*, 2023. 2

[63] Hanxun Yu, Wentong Li, Song Wang, Junbo Chen, and Jianke Zhu. Inst3d-lmm: Instance-aware 3d scene understanding with multi-modal instruction tuning, 2025. 3

[64] Yu-Jie Yuan, Yang-Tian Sun, Yu-Kun Lai, Yuewen Ma, Rongfei Jia, and Lin Gao. Nerf-editing: geometry editing of neural radiance fields. In *Proceedings of the IEEE/CVF conference on computer vision and pattern recognition*, pages 18353–18364, 2022. 3

- [65] Hang Zhang, Xin Li, and Lidong Bing. Video-llama: An instruction-tuned audio-visual language model for video understanding. *arXiv preprint arXiv:2306.02858*, 2023. 3
- [66] Longwen Zhang, Qiwei Qiu, Hongyang Lin, Qixuan Zhang, Cheng Shi, Wei Yang, Ye Shi, Sibei Yang, Lan Xu, and Jingyi Yu. Dreamface: Progressive generation of animatable 3d faces under text guidance. *arXiv preprint arXiv:2304.03117*, 2023. 3
- [67] Yunzhi Zhang, Zizhang Li, Matt Zhou, Shangzhe Wu, and Jiajun Wu. The scene language: Representing scenes with programs, words, and embeddings. In *Proceedings of the IEEE/CVF Conference on Computer Vision and Pattern Recognition (CVPR)*, pages 24625–24634, 2025. 2, 3

# VULCAN: Tool-Augmented Multi Agents for Iterative 3D Object Arrangement

## Supplementary Material

### 8. Comparison on Abstract Prompts

We demonstrate that our proposal can flexibly handle both abstract prompts (requiring model to decompose the task into action plans) and detailed multi-step instructions (requiring the model to faithfully execute instructions sequentially). Qualitative examples for both cases are provided in Fig. 10, Fig. 11, Fig. 12, and Fig. 13.

While the quantitative results for multi-step instructions are detailed in the main paper, we provide an additional quantitative comparison here using abstract instructions across 12 scenes. Unlike the multi-instruction setting where we evaluated all intermediate edited imagery, here we focus solely on the final output (i.e., the scene state after all edits are completed). We compare our approach against two baselines: BlenderAlchemy [26] and Blender-MCP [3]. As shown in Tab. 4, our model significantly outperforms all baselines.

Method	Coll.% $\downarrow$	Fl.% $\downarrow$	Plaus. $\uparrow$	Const. $\uparrow$
BlenderAlchemy [26]	0.500	0.333	3.433	2.833
Blender-MCP [3]	0.416	0.333	3.800	2.517
Ours	<b>0.000</b>	<b>0.000</b>	<b>4.000</b>	<b>3.383</b>

Table 4. **Evaluation on General Instructions.** Our model outperforms baselines and produces artifact-free outputs.

### 9. Details of the Multi-Tool Library

We provide detailed specifications of our multi-tool library, implemented using Blender’s Python API (bpy) [1]. We start with the visual API functions, followed by our collision-free solver, the constraint loss functions, and finally the collision/floating detector.

#### 9.1. Visual Probing Functions

The visual probing functions are iteratively called by the *Executor* agent to analyze the scene and select relevant objects or planes for arrangement. The library consists of three primary functions:

**LISTOBJECTSINAREA** returns the names of all objects within a specified image region. This is achieved by rendering an instance map of the scene, extracting all unique IDs from pixels within the input area, and retrieving the object names corresponding to those IDs.

**RAYPROBE** returns information regarding the first hitting point of a camera ray given its pixel coordinates. We implement this using bpy’s internal ray-casting function to

retrieve the position, the surface normal and the object name of the ray’s first hit. Additionally, this function extracts the planar surface of the object intersected by the ray. This is accomplished via a breadth-first traversal to identify all neighboring mesh faces of the intersected face that have surface normals within a cosine distance of 0.05.

**RENDERWITHHIGHLIGHT** generates a rendered image with selected objects highlighted in distinct colors. Similar to the previous functions, this process begins by rendering an instance map. Pixels corresponding to instance IDs in the selection list are then repainted with their assigned colors.

#### 9.2. Constraint Loss Functions

In the main paper, we proposed a set of constraints for the solver’s input. Here, we detail how each constraint is formulated as a differentiable loss.

**CLOSETOPIX** penalizes object placements that deviate from the provided pixel coordinates. Given the object’s 3D location  $\mathbf{p}$  and the normalized target pixel coordinates  $\mathbf{c}$ , the loss is calculated as:

$$\mathcal{L}_{c2p} = \lambda_{c2p} \|\mathbf{c} - \text{Proj}_C(\mathbf{p})\|_2^2, \quad (1)$$

where  $\text{Proj}_C(\cdot)$  denotes the camera projection function of camera  $C$ , and the weight parameter  $\lambda_{c2p}$  is set to 0.5.

**CONTACT** penalizes placements where the object fails to contact the target plane. Let the object’s plane and the target’s plane be defined by groups of vertices  $\mathbf{p}_{1,\dots,n}$  and  $\mathbf{q}_{1,\dots,m}$ , respectively, and the target plane’s normal direction denoted as  $\mathbf{n}$ . The loss consists of two components:  $\mathcal{L}_{\text{contact}}^{\text{touch}}$ , which enforces that the object’s plane touches the target plane; and  $\mathcal{L}_{\text{contact}}^{\text{above}}$ , which ensures the object’s plane resides fully on the outward side of the target plane. Mathematically, let  $\bar{q} = \max_{j=1,\dots,m}(\mathbf{q}_j \cdot \mathbf{n})$  denote the plane’s position along the normal direction. The losses are defined as:

$$\mathcal{L}_{\text{contact}}^{\text{touch}} = \min_{i=1,\dots,n} (|\bar{q} - \mathbf{p}_i \cdot \mathbf{n}|_1), \quad (2)$$

$$\mathcal{L}_{\text{contact}}^{\text{above}} = \frac{1}{n} \sum_{i=1,\dots,n} \text{Relu}(\bar{q} - \mathbf{p}_i \cdot \mathbf{n}), \quad (3)$$

$$\mathcal{L}_{\text{contact}} = \lambda_{\text{contact}}^{\text{touch}} \mathcal{L}_{\text{contact}}^{\text{touch}} + \lambda_{\text{contact}}^{\text{above}} \mathcal{L}_{\text{contact}}^{\text{above}}. \quad (4)$$

where  $\lambda_{\text{contact}}^{\text{touch}}$  and  $\lambda_{\text{contact}}^{\text{above}}$  are both set to 100. Note that the contact loss also applies to non-parallel planes.

**NOOVERHANG** enforces that the object is placed within the bounds of the target plane. While objects can typically be placed fully within the target surface (e.g., a book

on a shelf), certain scenarios (e.g., stacking books) may require part of the object to overhang. To address this, we developed two modes for this loss: *full* mode, which penalizes any part of the object’s plane extending beyond the target’s convex hull; and *center-only* mode, which only evaluates the center of the object’s plane. We first project the vertices of both planes ( $\mathbf{p}_{1,\dots,n}$  and  $\mathbf{q}_{1,\dots,m}$ ) onto the target plane’s 2D space (denoted as  $\hat{\mathbf{p}}$  and  $\hat{\mathbf{q}}$ ). We then determine if any  $\hat{\mathbf{p}}$  lies inside the convex hull  $\hat{\mathbf{q}}_{1,\dots,m'}^{cvx} = \text{ConvexHull}(\hat{\mathbf{q}}_{1,\dots,m})$  by applying a cross-product examination with the convex hull’s edges  $\hat{\mathbf{e}}_i = \hat{\mathbf{q}}_{i+1}^{cvx} - \hat{\mathbf{q}}_i^{cvx}$ . The two modes are defined as:

$$\mathcal{L}_{OH}^{full} = \lambda_{OH} \max_{i,j} (\text{ReLU}((\hat{\mathbf{p}}_i - \hat{\mathbf{q}}_j^{cvx}) \times \hat{\mathbf{e}}_j)), \quad (5)$$

$$\begin{aligned} \mathcal{L}_{OH}^{center} = \lambda_{OH} \max_j & (\text{ReLU}((\text{avg}(\hat{\mathbf{p}}) - \hat{\mathbf{q}}_j^{cvx}) \times \hat{\mathbf{e}}_j)) \\ & + \lambda_{OH}^{align} \|\text{avg}(\hat{\mathbf{p}}) - \text{avg}(\hat{\mathbf{q}}^{cvx})\|, \end{aligned} \quad (6)$$

where  $\lambda_{OH}$  and  $\lambda_{OH}^{align}$  are set to 20 and 1, respectively. In the *center-only* mode, an additional  $L_2$  loss between the centers of the two planes is applied to encourage placement near the target plane’s center. In practice, the agent selects the mode via an argument in the NOOVERHANG constraint. If *full* mode is selected, only the first formulation is applied. Otherwise, the solver first attempts to solve using *full* mode and switches to *center-only* mode if no solution is found.

**DISTANCE** constrains the distance between two objects to be close to a target value,  $dist$ . This is implemented as an  $L_2$  loss between  $dist$  and the Euclidean distance between the centers of the two objects:

$$\mathcal{L}_{dist} = \lambda_{dist} \|\mathbf{x}_o - \mathbf{x}_{tgt}\|_2^2, \quad (8)$$

where  $\mathbf{x}_o$  and  $\mathbf{x}_{tgt}$  represent the positions of the placed object and the target object, respectively, and  $\lambda_{dist}$  is set to 0.3.

**FACETo** enforces that an object faces a specific target object, plane, or camera. Let  $\mathbf{v}_o$  denote the object’s facing direction and  $\mathbf{v}_{tgt}$  the target facing direction. The loss is calculated as the cosine distance between  $\mathbf{v}_o$  and the projection of  $\mathbf{v}_{tgt}$  onto the object’s azimuth plane. Letting  $\mathbf{u}_o$  be the up vector of the object, the loss is defined as:

$$\mathcal{L}_{FT} = \lambda_{FT} \text{CosDist}(\mathbf{v}_o, \mathbf{v}_{tgt} - \text{SG}((\mathbf{u}_o \cdot \mathbf{v}_{tgt}) \mathbf{u}_o)), \quad (9)$$

where SG denotes the stop-gradient function, and  $\lambda_{FT}$  is set to 0.5. Analogously, we implement a **BACKTo** constraint using the same formulation to align the object’s back with the target.

**ROTATE** explicitly sets the object’s rotation to a specific degree. This is achieved by setting the initial rotation angle of the object to the input degree and fixing it during the optimization process. This constraint is deactivated if any **FACETo/BACKTo** constraint is present.

### 9.3. Collision-Free Solver

As outlined in Algorithm 1 of the main paper, the solver first perturbs the target pixel coordinates in the **CLOSETOPIX** constraint with a fixed standard deviation of 0.2, generating a batch of variant coordinates. It then optimizes a batch of target poses corresponding to each perturbed coordinate.

The positions are initialized at the first intersection point of a ray cast from the pixel coordinates, as determined by the **RAYPROBE** function. Initial rotation angles are set to zero, unless a **ROTATE** constraint is explicitly present. We employ the AdamW optimizer for 800 iterations, with a learning rate initialized at  $1e-1$  and linearly decayed to  $1e-4$ . To simplify the optimization, we fix the rotation along the pitch and roll axes, optimizing only the rotation around the vertical (yaw) axis.

Upon completion, we re-evaluate the loss for each solution in the batch using the original, unperturbed coordinates for the **CLOSETOPIX** target. Solutions exceeding a loss threshold of  $1e-1$  are discarded.

Finally, we assess the remaining solutions for collisions, processing them in ascending order of error. Since the standard Blender Python API (bpy) does not expose the native physics engine’s collision detection, we leverage geometry modifiers to approximate this. Specifically, we first apply a **SOLIDIFY** modifier to inflate the meshes, ensuring robust detection for thin structures such as walls or floors. Then, we convert the source and target objects into manifold meshes via the **REMESH** modifier. We then employ a **BOOLEAN** modifier to compute the intersection volume between objects. A collision is declared if the intersection geometry penetrates the object’s bounding box above a threshold of 0.01. The first solution found to be collision-free is selected as the final output. Figure 8 illustrates the modifiers in Blender, and demonstrates how our detector effectively calculates intersection volumes.

### 9.4. Floating Detection

Upon completion of the object arrangement, we conduct a floating check on all objects within the scene. This is implemented by casting a ray from the center of the bottom face of the object’s bounding box. If the ray intersects another object within a distance of 0.01, the object is classified as grounded (i.e., not floating). The validation passes only if all objects that were grounded in the initial state remain grounded in the edited scene.

## 10. Prompts for Agents

**Planner.** We employ distinct prompting strategies for general instructions and per-step instruction settings. For general instructions, we prompt the planner to autonomously generate a plan based on the current state and historical steps. To prevent infinite loops, we impose a max-

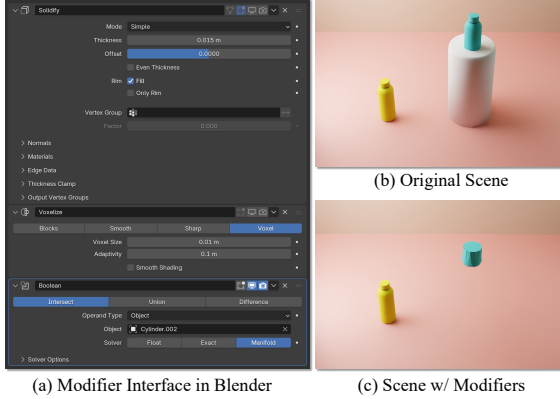


Figure 8. **Collision Detector.** (a) Configuration of our collision detector, consisting of three modifiers with parameter settings as illustrated. (b-c) Visualization of the intersection: upon activation, the modifiers extract the collision geometry, i.e. the portion of the bottle below the cylinder’s surface.

imum step limit for each task, typically ranging from 3 to 6 steps. The model is required to make a feasible plan within this constraint; if the estimated steps exceed this limit, the attempt is automatically classified as a failure.

In the detailed per-step instruction setting, the model is prompted to read the current instruction, analyze it within the global context (considering both past and future steps), and rewrite it such that the locally-operating *Executor* can execute it based solely on the current state. Figures 17 and 18 illustrate the prompts for the general instruction setting, while Fig. 19 shows the prompt for the detailed setting.

**Executor.** The prompt for the executor is presented in Fig. 20 and Fig. 21. Supplementing this, we provide API documentation (as shown in Fig. 16) for the visual tools, enabling the model to understand the functionality of each function and the definitions of their parameters.

**Evaluator.** Figure 22 shows the *Evaluator* prompt. This agent accepts the rendered image of the edited state and the instruction from the *Planner* instruction to assess the edit’s plausibility and correctness. In practice, we implement an early termination for efficiency: If all *Evaluators* assign a *good* or *excellent* verdict to the current edit, we accept it as the result for that step and skip remaining attempts.

**Benchmark Judges.** In addition to the multi-agent pipeline, we provide the judge prompt used in our benchmark (Fig. 23), which is adapted from experiments in FirePlace [27]. This agent examines the results of all steps collectively, evaluating them within a global context to assign scores for each step. For each data sample, we employ 5 benchmark evaluators and report the average scores.

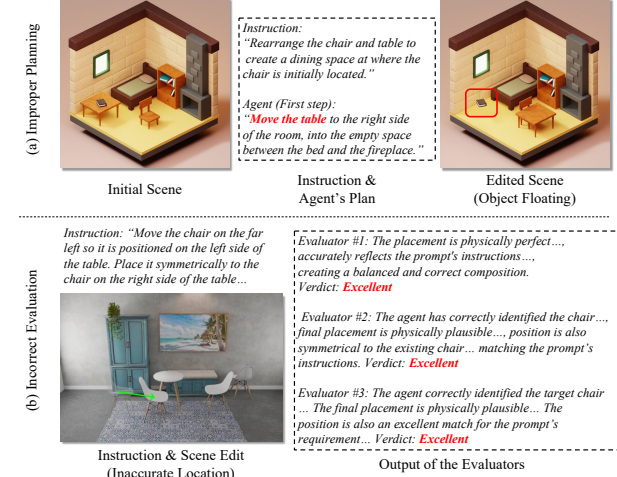


Figure 9. **Failure Cases.** Top: The *Planner* generates an improper plan (i.e., moving the table before clearing it), resulting in floating artifacts. Bottom: All three *Evaluators* provide false positive verdicts despite of the arrangement deviating from the instruction.

## 11. Adaptive Backtracking

Algorithm 2 presents detailed pseudocode for the adaptive backtracking mechanism employed within our search framework.

**Algorithm 2:** Plan Search with Adaptive Backtracking SEARCH

**Parameter:** Object arrangement pipeline  $\mathcal{F}$ , maximum allowed steps  $s_{max}$ , user instruction  $T$ .

**Input:** Previous scenes  $\mathcal{S} = \{S_{0, \dots, k-1}\}$ , current step  $k$ , anchor depth  $d_a$ , current maximum depth  $d_{max}$ .

**Output:** A sequence of edited scenes  $S_{0, \dots, k}$ .

$/*$  Run model for current step.  $*/$   
 $state, S_k \leftarrow \mathcal{F}(\mathcal{S}, T, k);$

**if**  $state = "Complete"$  **then**

$/*$  Search is complete.  $*/$

**return**  $\mathcal{S}$ ;

**else if**  $k < s_{max}$  &  $state = "Edited"$  **then**

$/*$  Current step is done.  $*/$

**if**  $k + 1 > d_{max}$  **then**

$/*$  Reaches a breakthrough. Update anchor depth.  $*/$

$d_{max}, d_a \leftarrow k + 1;$

$\text{SEARCH}(\mathcal{S} \cup \{S_k\}, k + 1, d_a, d_{max});$

**else**

$/*$  Failed. Backtracking.  $*/$

$d_a \leftarrow d_a / 2;$

$\text{SEARCH}(\{\mathcal{S}_{0, \dots, d_a - 1}\}, d_a, d_a, d_{max});$

## 12. Additional Discussion on Failure Cases

Our model significantly enhances the backbone MLLM’s capability for iterative object arrangement. However, despite robust design components, the system still can be affected by the inherent limitations of the backbone MLLM, as shown in Fig. 9.

A primary failure mode is planning error. The MLLM may generate an incorrect plan for the current step, resulting in infeasible solutions. While our backtracking algorithm enables recovery from such errors, this trial-and-error process significantly impacts the model’s efficiency.

Secondly, as noted in the main paper, the *Evaluator* may occasionally yield false positives (i.e., validating an erroneous arrangement) due to MLLM hallucinations. Although our polling mechanism mitigates this risk, there remains possibilities that the *Evaluators* will reach a consensus on an incorrect verdict. While future advancements in MLLMs may eliminate these issues, we believe that developing more robust evaluation agents for current MLLMs represents a promising direction for future research.

## 13. Additional Results

We provide supplementary visual results, including qualitative comparisons against baseline methods and extended demonstrations of our model’s performance.

**Additional Qualitative Comparisons.** We present further visual comparisons with baseline methods. Figures 10 and 11 illustrate four examples under the per-step instruction setting, while Figures 12 and 13 shows four examples using general instructions.

**Additional Results.** Figures 14 and 15 display additional results generated by our method under per-step and general instruction settings, respectively.

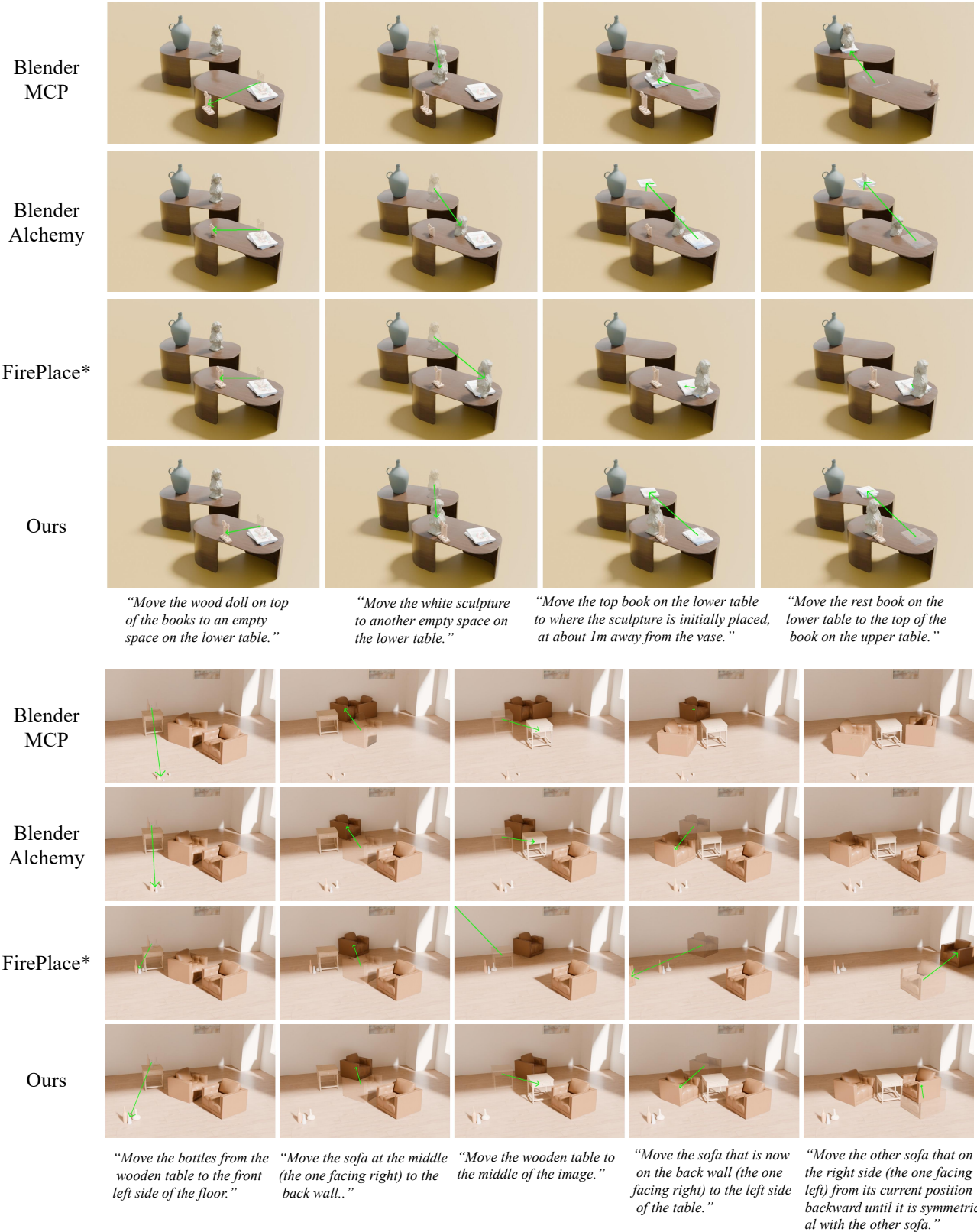


Figure 10. **Comparison on Per-step Instruction Examples.** The input per-step instructions are shown below the images.

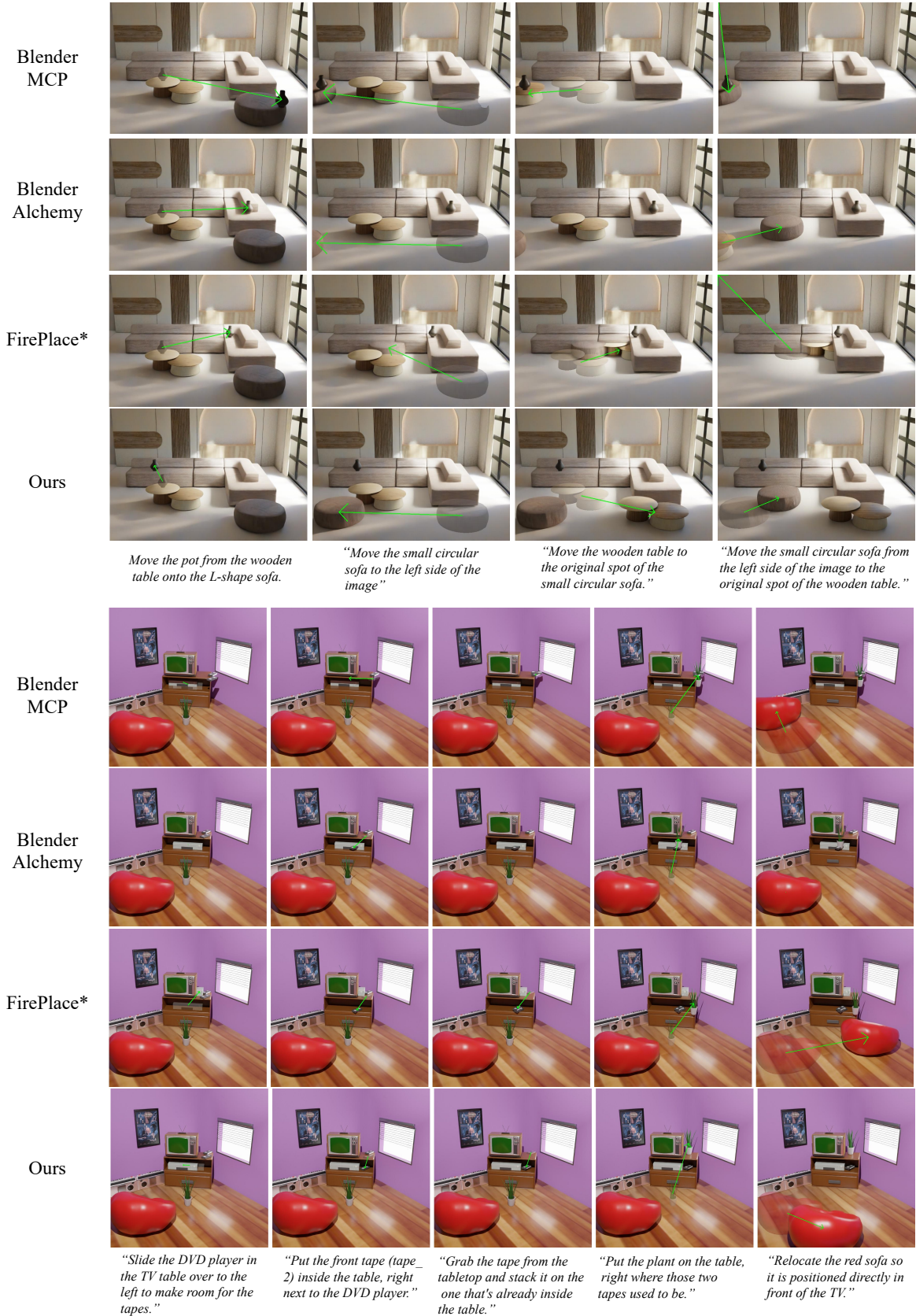
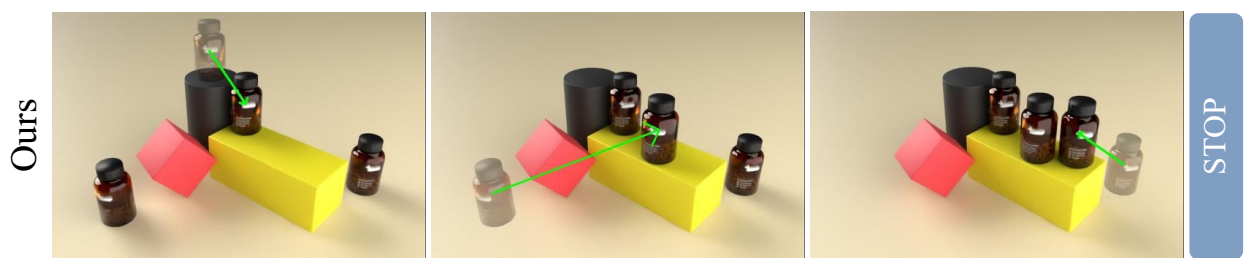
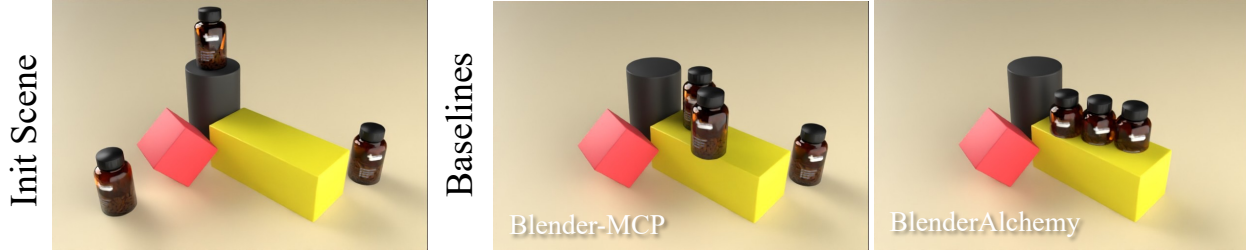


Figure 11. Comparison on Per-step Instruction Examples (cont'd).

Instruction: Can you place all three bottles on the yellow block?



Agent:  
Move the bottle that is currently on top of the black cylinder onto the yellow block.

Agent:  
Place the bottle from the left side of the scene onto the yellow block, next to the bottle that is already there.

Agent:  
Place the last bottle on the right on to the yellow block, next to the other two bottles.

Instruction: Move the long table to the front of the shelf, where the chair and plant is located at.



Agent:  
Move the chair to the empty space in the bottom-left corner of the room.

Agent:  
Move the plant to the empty space on the floor to the right of the shelf.

Agent:  
Move the long table to the front of the shelf.

Figure 12. **Comparison on General Instruction Examples.** The input instruction is shown at the top. We show the initial scene, baseline results, and our model’s step-by-step outputs. The plans generated by our model are listed below the edited images.

Instruction: Can you move the tea saucer on top of the book?

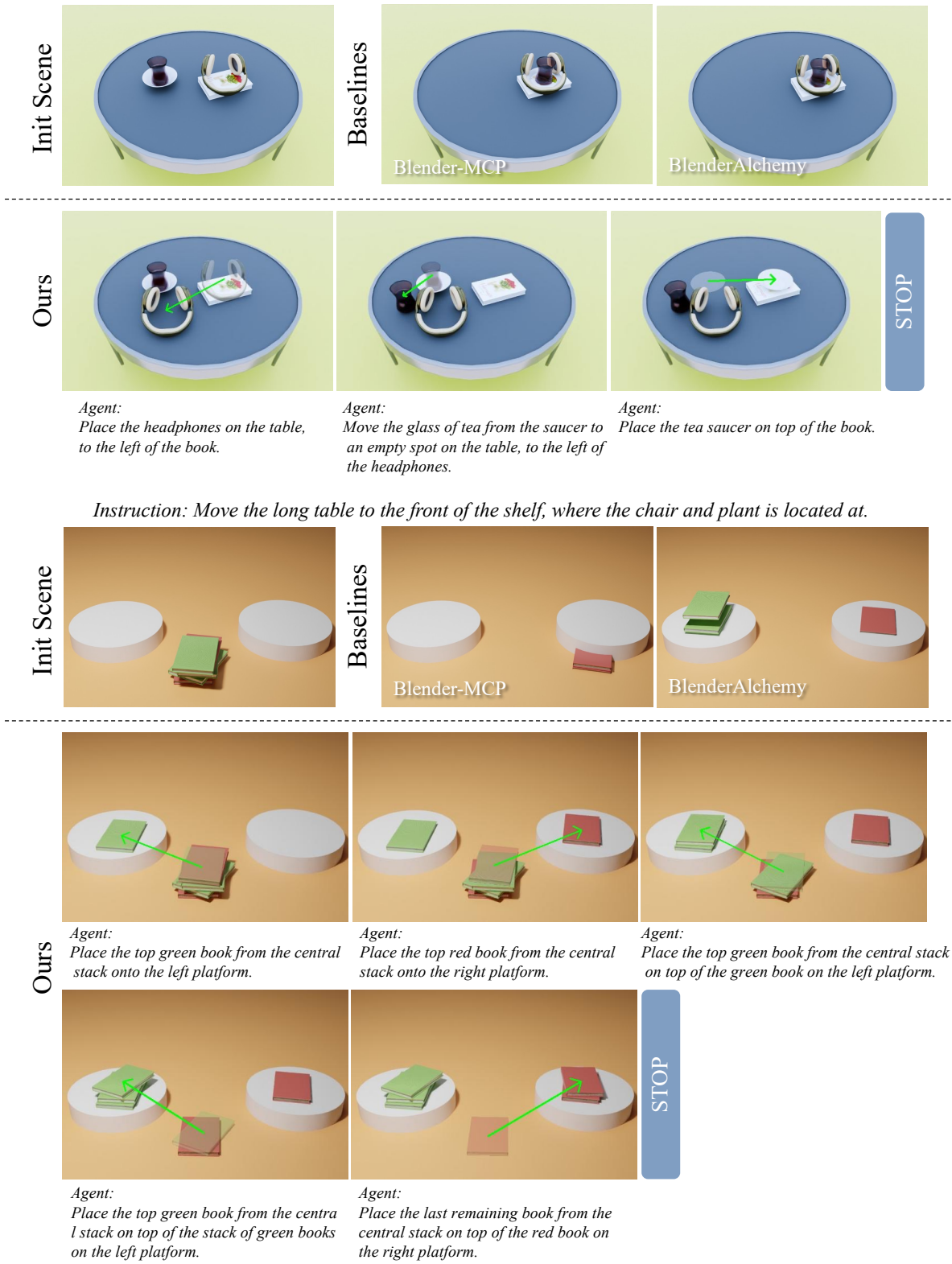


Figure 13. Comparison on General Instruction Examples (cont'd).

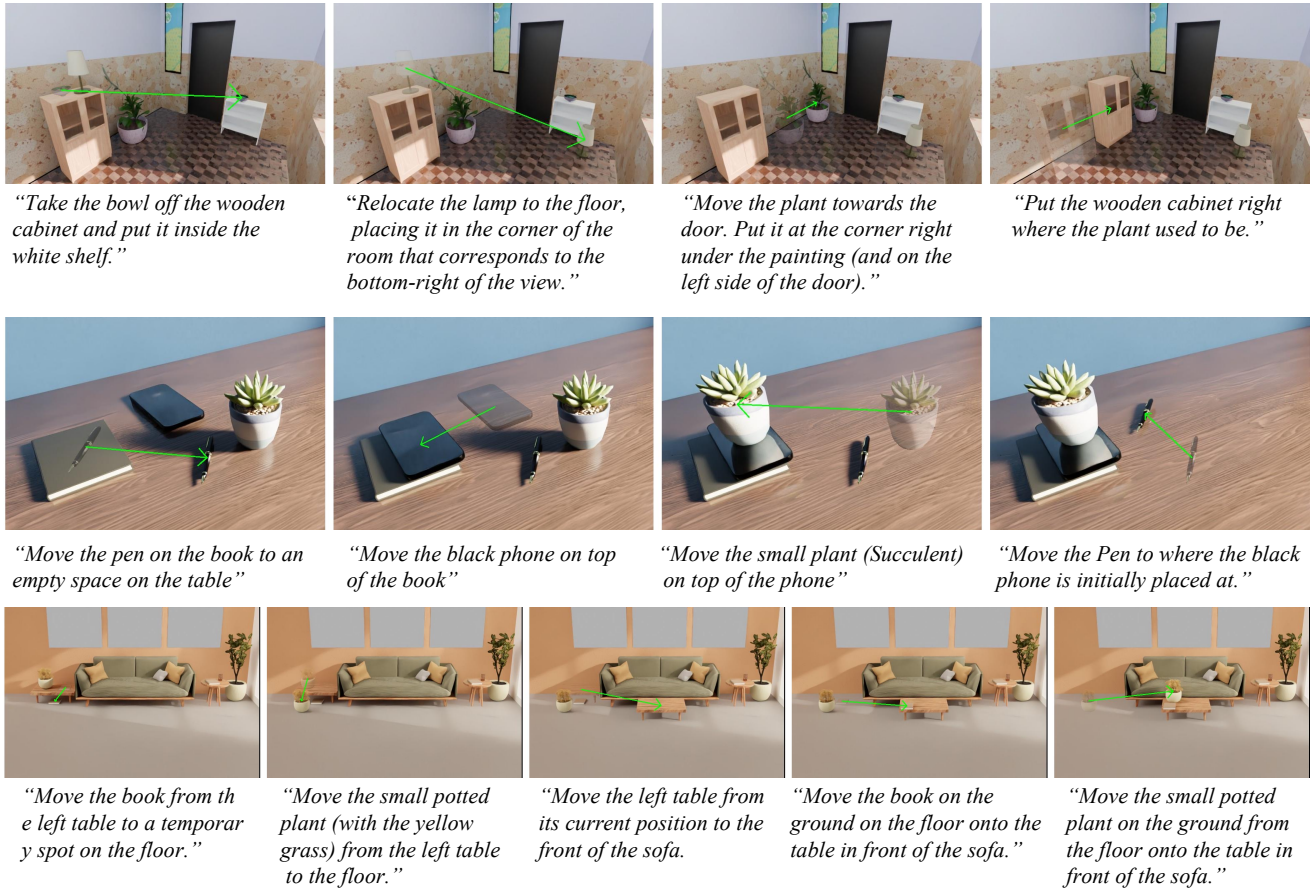


Figure 14. **Additional Results on Per-step Instruction Examples.** The input instructions are shown below the images.

Instruction: Switch the position of the small round sofa and the wooden table.



STOP

Agent:  
Move the vase from the table and place it on the floor to the left of the tables.

Agent:  
Move the small round sofa to a temporary position in the empty space on the floor in the bottom-left area.

Agent:  
Move the larger of the two wooden tables to the empty space in the bottom-right corner of the room, where the small round sofa was originally located.

Agent:  
Move the small round sofa to the now-empty spot where the larger wooden table was originally located, next to the smaller wooden table.

Instruction: Move the two chairs to the empty space in front of the shelf, then move the table on the upper left (the one without the book on it) to where the two chairs are originally located at.



STOP

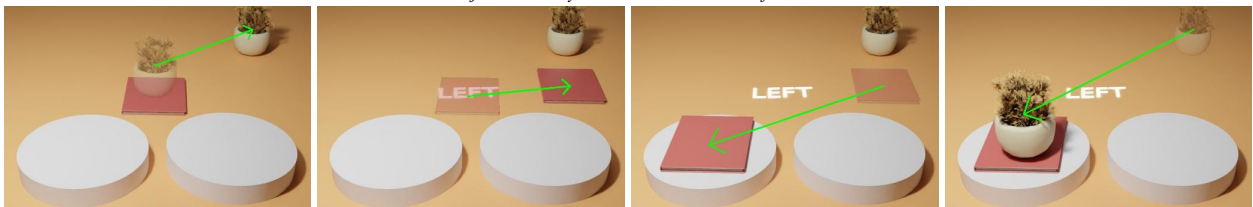
Agent:  
Move the leftmost chair to the empty space on the right, in front of the bookshelf.

Agent:  
Move the remaining chair to the empty space in front of the shelf, placing it next to the chair that was already moved.

Agent:  
Move the printer from the desk and place it on the empty floor space to the left of the desk.

Agent:  
Move the empty desk on the left to the empty space behind the other desk, centering it in the area where the two chairs were originally located.

Instruction: Move the book and the plant to elsewhere to reveal the text below, then place the two objects to the cylinder as the text on the floor instructed.



STOP

Agent:  
Move the plant to a temporary empty space on the floor.

Agent:  
Move the red square object to an empty space in the top-right area of the floor to reveal the text underneath it.

Agent:  
Place the red square object on top of the left cylinder.

Agent:  
Place the plant on top of the red square.

Figure 15. **Additional Results on Per-Step Instruction Examples.** The input instructions are shown above the images, while the plans generated by the *Planner* agent are shown below.

```

def ray_probe_for_plane(coord_list):
"""
Casts rays from specified camera-view coordinates and reports the first object intersected by
each ray. It also extract the plane from the hitting point.

Args:
- coord_list: A list of normalized 2D coordinates (x, y) (from 0.0 to 1.0) from which to cast
  rays. Example: [[0.25, 0.25], [0.75, 0.75]]

Returns:
- hit_info_list: A list of hit details, one for each input coordinate. Each item in the list
  will be: A tuple containing (hit_object_name, hit_location_3d, hit_normal_vector) if an
  object was intersected. None if the ray did not intersect with any object.

"""

def render_with_highlighted_object(output_path, object_name_list, object_color_list=None):
"""
Renders an image with specified objects highlighted by semi-transparent colored masks. This is
useful for visually identifying objects in the rendered output.

Args:
- output_path: The file path to save the rendered image.
- object_name_list: A list of up to 10 object names to highlight. Example: ["Cube", "Sphere"].

Returns:
- image: The rendered Image object.
- object_color_dict: A dictionary mapping each object name to its corresponding highlight color
  in the image. Please note that the highlight color does not indicate the original color of
  the object.

"""

def list_all_object_in_view(interested_area="[0,0,1,1]"):
"""
Lists all objects visible within a specified rectangular area of the camera's view.

Args:
- interested_area: A list of four normalized coordinates x1,y1,x2,y2 (from 0.0 to 1.0) defining
  the rectangular area to check. Example: [0.25, 0.25, 0.75, 0.75]

Returns:
- object_list: A list of names of the objects found within the specified area.

"""

```

Figure 16. **Description of Visual API functions.** Note that function names may differ from those in the main text.

[[Task Description]]

You are an AI 3D object arrangement planner to solve a multi-step arrangement task.

Given a user's instruction and a history of edit images from your predecessors,  
plan the (current) arrangement step.

Inputs:

1. General Instructions: The instruction from the user to define the task.
1. Previous Edits: Description of edits made by predecessors.
2. Image History: A sequence of images: [initial scene, result\_of\_step\_1, ..., result\_of\_latest\_step, current scene]. Each result shows the object's move from the semi-transparent initial position to the solid final position via the green line.
3. Maximum Allowed Steps: The maximum number of steps allowed for the task.

Note:

- \* All directions (e.g., "left," "top") are relative to the 2D image.
- \* All 2D coordinates are in normalized (x, y) format.
- \* Make your answer as concise as possible.
- \* Only one object can be operated on per step. Avoid creating plans that arrange multiple objects.
- \* After each arrangement, no object in the scene should be colliding with others or floating (except the already floating ones).
- \* To move an object with other objects on it, you should first remove the stacked objects to prevent them floating after the movement.

Your Tasks:

1. Summarize History:

Briefly describe the initial scene and all previous edits based on the History Images.

2. Predict Future Steps:

Plan the future arrangement (placement and rotation) steps based on the complete image history and the user's general instruction for global planning.

If you believe the goal is already achieved, output a <finished> token and skip all remaining steps.

If you believe the goal is impossible to reach within the maximum allowed steps (including those already taken), output an <impossible> token and skip all remaining steps.

Otherwise, briefly describe your future plan.

3. Updated Instruction:

Provide an [updated\_instruction] block. Output your local instruction for the current step, It should reference only the latest\_scene (e.g. remove all "initial position" prompts). Add details in the instruction so it is unambiguous.

Make sure all metric information (e.g., 0.5m, 20cm), object name information (e.g. Chair\_000), and orientation information (e.g. facing towards another object) in the original instruction is retained and unchanged.

Figure 17. Prompt for the *Planner* with General Instructions (Part 1).

#### 4. Target Coordinate:

Select the single coordinate where the object's <center/bottom/> should be placed to best fit the Current Instruction, and does not collide with other objects.

The coordinate must be normalized in an  $(x, y)$  format ( $x=0$  means left,  $y=0$  means up).

Output the coordinate information in a [coordinate] block.

#### Example Output:

The initial scene contains a table with a teacup, a spoon, and a book on it.

There're two previous arrangements in total.

arrangement 1: The teacup was moved on top of the book.

arrangement 2: The spoon was moved inside of the teacup.

(If the goal is already achieved)

The goal is already achived. <finished>

(If the goal is not achieved and require more steps)

The goal is to place the pen to the apple's original location, and facing to the banana. From the current state, this requires a 2-step plan:

1. move the apple to an empty space

2. Place the pen to apple's original position (from image 1,  $\approx(0.52, 0.56)$ ), and facing to the banana.

(If allowed steps are sufficient)

The maximum allowed steps is 5. Since this plan only requires 2 more steps (4 steps in total), it is valid.

[updated\_instruction]

Place the pen to the the table, and facing the banana.

[end\_of\_updated\_instruction]

[coordinate]

The center of the object should be around [0.52, 0.56].

[end\_of\_coordinate]

(If allowed steps are insufficient)

The maximum allowed steps is 3. Since this plan requires 2 more steps (4 steps in total), it is impossible to reach the goal.

<impossible>

(the input instructions and images)

Figure 18. Prompt for the *Planner* with General Instructions (Part 2).

[[Task Description]]

You are an AI 3D object placement planner.

Given a list of instructions and a history of scene images,  
plan the (current) placement step.

Inputs:

1. Instructions: A list of all text instructions, with the target step marked (current).
2. Image History: A sequence of images: [initial scene, result\_of\_step\_1, ..., result\_of\_latest\_step, current scene].  
Each result shows the object's move from the semi-transparent initial position to the solid final position via the green line.

Note:

- \* All directions (e.g., "left," "top") are relative to the 2D image.
- \* All 2D coordinates are in normalized (x, y) format.
- \* Make your answer as concise as possible.

Your Tasks:

1. Summarize History:

Briefly describe the initial scene and all previous edits based on the History Images and Previous Instructions.

2. Reasoning:

Plan your placement for the (current) instruction with both the all historic images and future instructions for global planning.

3. Updated Instruction:

Provide an [updated\_instruction] block. Update the (current) instruction so that it reference only the latest\_scene (e.g. remove all "initial position" prompts). Add details in the updated instruction so it is unambiguous. Make sure all metric information (e.g., 0.5m, 20cm) and object name information (e.g. Chair\_000) in the original instruction is retained and unchanged.

4. Target Coordinate:

Select the single coordinate where the object's <center/bottom/> should be placed to best fit the Current Instruction, and does not collide with other objects. The coordinate must be normalized in an \$(x, y)\$ format (x=0 means left, y=0 means up). Output the coordinate information in a [coordinate] block.

Example Output:

The initial scene contains a table with a teacup, a spoon, and a book on it.

Placement 1: The teacup was moved on top of the book.

Placement 2: The spoon was moved inside of the teacup.

Reasoning: Current instruction targets the pen's original location (from image 1, \$\approx(0.52, 0.56)\$).

A future instruction ("place a banana next to the apple") requires leaving space.

I will place the apple at the original pen's spot, ensuring room for the banana.

[updated\_instruction]

Place the apple on the table to the left of the teacup, and leave a small gap for a banana to be placed next to it.

[end\_of\_updated\_instruction]

[coordinate]

The center of the object should be around [0.52, 0.56].

[end\_of\_coordinate]

(the input instructions and images)

Figure 19. Prompt for the *Planner* with Per-step Instructions.

#### [[Task Description]]

As a Virtual Set Dresser AI, your task is to plausibly place a specified object within a 3D Blender scene based on a user's prompt.

#### [Inputs]

1. Target Prompt: The objective for the scene (e.g., "Place the vase on the desk").
2. Initial Image: The view of the initial scene.
3. Blender Tools: A suite of functions for scene interaction.

#### [General Principles]

- \* Strictly follow the steps, do not skip any of them unless it's explicitly mentioned in the prompt.
- \* Please be efficient with your function calls. Consolidate function usage where possible.
- \* Stop immediately after providing the final confirmation message. DO NOT evaluate your own result.
- \* Log your full thoughts, the reasoning for every tool call.

#### [Task Specific Principles]

- \* All directions are relative to the image. For example, 'left' means the left side of the image as you see it.
- \* DO NOT make assumptions about the Blender's coordinate system (e.g. X-axis means left/right; Z=0 means the floor plane).
- \* All 2d coordinates (e.g. [0.43, 0.62]) are in the \$(x, y)\$ format.
- \* DO NOT rely on the object's full name to determine its property, instead exam more on the image visually.
- \* DO NOT use object's name as planes in the constraint parameters. Always use bounding box planes or created planes.
- \* DO NOT use type of constraint that not supported by the description list.

#### [Constraint Description]

The following constraints are supported:

- \* `ObjectName("<name_of_object>")`: The target object. Make sure it is called only once.
- \* `Contact("down/side/up", "<name_of_surface>")`: The bottom/side/top of the target object contacts the surface.
- \* `NoOverhang("down", sur, mode)`: 'full\_only' means the object's bottom is completely within the surface, while 'center' means the center of the bottom is on the surface.
- \* `CloseToPix("center"/"down", [x, y])`: The object's center/bottom is close to the 2D pixel coordinate in the camera view.
- \* `Distance("<name_of_other_object>", <distance>)`: The distance (in meters) between the center of the target object and another object. Use it when the instruction contains distance information.
- \* `FaceTo("<name_of_object>/<name_of_surface>/camera")`: The object should face to the center of an object / the normal of the surface / camera.
- \* `BackTo("<name_of_object>/<name_of_surface>/camera")`: The object should back to the center of an object / the normal of the surface / camera.
- \* `Rotate(90/180/270)`: Rotate the object by 90/180/270 degrees. This constraint will be overridden by FaceTo/BackTo.

There're two types of plane names allowed:

- \* `<object_name>_<face_id>`: Planes created by `ray_probe_for_plane` calls.
- \* `<object_name>_<up>`: The top surface of the object. Use this plane for stacking objects on top of each other.

Figure 20. **Prompt for the Executor (Part 1)**.

[Workflow]

IMPORTANT: You must finish the task by following these steps in strict order.

Step 1: Visual Scene Analysis

Analyze the prompt and initial image to identify the target object, its destination, and key reference objects.

\* Hint 1: Use the ray\_probe tool on likely image coordinates to determine precise 3D coordinates and identify reference objects. You can probe multiple points for comprehensive data.

\* Hint 2: Use list\_all\_object\_in\_view on interested area to retrieve relevant objects for placement in a certain area.

\* Hint 3: (Only when the previous hints are not sufficient) use render\_with\_highlighted\_object to visually identify and confirm relevant objects for placement. DO NOT use this function when the input instruction contains color information (e.g. red book).

Step 2: Plane Selection

Find the plane that the object should be placed on (or hanged to). Use the ray\_probe\_for\_plane tool on likely image coordinates to extract the plane's name located at the coordinate.

In addition to the suggested coordinates, you are encouraged to explore other pixels to find the right plane to place the object. Please carefully look at the image and find best candidates for plane selection.

Step 3: Design constraints for the placement solver

Based on your visual analysis, and the description of the constraint list, design a set of constraints that helps the solver to solve the right position for placement. Output the constraints in the [constraints] block and end with a <completion> token. For NoOverHang constraints, use "full\_only" for large surfaces (table, floor) and "center" for small surfaces (book, block).

Constraint List Requirements:

\* Strictly follow the constraint syntax from the description.

\* Must include at least one CloseToPix constraint.

\* All included plane names must be valid (from Step 2 or the object's bounding box).

Example Output:

```
[constraints]
["ObjectName", "<Name_of_the_moved_object>"],
["CloseToPix", "center", [0.5, 0.5]],
["Contact", "down", "<Name_of_surface_from_step_2>"],
["NoOverhang", "down", "<Name_of_surface_from_step_2>", "full_only"],
<rotation_constraint_example>
[end of constraints]
<completion>
```

[[End of Task Description]]

(the input instructions and images)

Figure 21. **Prompt for the Executor (Part 2).**

[[Task Description]]

You are a Virtual Set Dresser AI. Your task is to evaluate the plausibility and correctness of an object's final placement.

You are given two inputs:

1. Target Prompt: The text instruction for the placement. All directions described in the text are relative to the image.
2. Edited Image: A render showing the object's move from the semi-transparent initial position to the solid final position via the green line.

Please strictly evaluate the final placement in the edited image against the target prompt. Check carefully for any physical errors (floating, clipping) or positional inaccuracies. Provide a verdict (<excellent|good|fair|bad|terrible>) with a clear justification in an [evaluation] block,

\* Example:

[evaluation]

visual\_exam: The agent correctly identified the support surface but failed on two counts: the object is visibly floating, and its position does not match the prompt's request to be in the corner.

verdict: fair

[end of evaluation]

[[Evaluation Rubric]]

Excellent: Perfect placement. Physically plausible (no errors) AND location exactly matches the prompt.

Good: Physically perfect placement, but the location is only an approximation of the prompt (e.g., near the corner, not on it).

Fair: Has one clear flaw:

A) Correct location, but minor physics error (slight floating/clipping).

B) Physically plausible, but wrong location on the correct surface.

Bad: Has multiple flaws OR one severe flaw:

A) Wrong location and a physics error.

B) Placed on the wrong support surface (e.g., floor instead of table).

Terrible: Physically impossible (e.g., floating in mid-air) or shows a complete misunderstanding of the prompt.

(the input instruction and images)

Figure 22. **Prompt for the Evaluator.**

Your task is to evaluate a sequence of AI-generated object placements based on their realism and consistency with instructions.

Here's the instruction for the previous agent (each line corresponds to one step):  
(user's instruction)

The input image showing the render of the initial scene and all edited scenes for each step (from left to right).  
(All input images)

Please STRICTLY evaluate each result image (starting from '"0") on two separate criteria using the scale:  
'<excellent|good|fair|bad|terrible>'.

1. **Plausibility:** How physically realistic is the placement?
2. **Correctness:** How well does the placement match the agent's instruction?

#### ### Evaluation Rubric

- \* **Excellent:** Perfect placement. Physically plausible AND location exactly matches the prompt.
- \* **Good:** Physically perfect placement, but the location is only an approximation of the prompt.
- \* **Fair:** Has one clear flaw:
  - \* A) Correct location, but minor physics error (slight floating/clipping).
  - \* B) Physically plausible, but wrong location on the correct surface.
- \* **Bad:** Has multiple flaws OR one severe flaw:
  - \* A) Wrong location and a physics error.
  - \* B) Placed on the wrong support surface (e.g., floor instead of table).
- \* **Terrible:** Physically impossible (e.g., floating in mid-air) or shows a complete misunderstanding of the prompt.

#### ### Output Format

Provide your ratings and justifications as a single JSON object. **DO NOT** output anything other than the JSON object.

\*Example:\*

```
```json
{
  "0": {
    "correctness": "fair",
    "plausibility": "bad",
    "justification": "Placed on the correct table but in the wrong spot, and the object is clearly clipping into the wall."
  },
  "1": {
    "correctness": "excellent",
    "plausibility": "excellent",
    "justification": "Perfect placement, exactly matching the instruction."
  }
}
```

Figure 23. Prompt for the Benchmark Judges.